Advances in Nano Research, *Vol. 11, No. 3 (2021) 251-269*
https://doi.org/10.12989/anr.2021.11.3.251

Effect of three-dimensional thermal stresses on torsional vibration of cracked nanorods surrounded by an elastic medium

Sardar S. Abdullah[1,2b], Shahrokh H. Hashemi[**1,3], Nazhad A. Hussein[2a] and Reza Nazemnezhad[*4]

[1]*School of Mechanical Engineering, Iran University of Science and Technology, Narmak, Tehran, 11369, Iran*
[2]*Mechanical Department, College of Engineering, Salahaddin University-Erbil, Erbil, 44001, Iraq*
[3]*Center of Excellence in Railway Transportation, Iran University of Science and Technology, Narmak, 11369, Tehran, Iran*
[4]*School of Engineering, Damghan University, Damghan, Islamic Republic of Iran*

(*Received September 30, 2020, Revised June 16, 2021, Accepted June 29, 2021*)

Abstract. The effect of thermal stresses on the torsional vibration of non, single, and double-cracked nanorods surrounded by an elastic medium is investigated. The differential constitutive relation of the nonlocal theory is applied to the motion equation. Three-dimensional linear thermal strains raised from the thermal stresses are derived using nonlinear Green's strains. The surrounding elastic medium acts as infinite torsional springs. The crack is modeled as a rotational spring. Using Hamilton's principle, the motion equation is obtained. Effect of the crack position and severity, number of cracks, high and low temperatures, nonlocal coefficient, elastic medium stiffness, and nanorod length are examined. The temperature effect on the frequencies depends on the values of the crack parameters, crack numbers, elastic medium stiffness, and nanorod length, and it is independent of the nonlocal scale coefficient. The crack leads to a decrease in the frequencies at any temperature. The elastic medium causes an increase in the frequencies at any temperature.

Keywords: crack; elastic medium; thermal stresses; torsional vibration

1. Introduction

The static and dynamic characteristics of any structure depend on the size of the structure. The nanostructures and nanoscale elements possess extraordinary electrical, thermal, and mechanical properties, and investigation of their static, dynamics, and thermal behaviors has been recently conducted by several researchers. The nanostructures and nanoscale elements can be used to produce and design many new materials and devices with a wide range of applications, such as nanomedicine, nanoelectronics, and biomaterials energy production. The classic theories can be applied to the structures in macroscales while for the micro or nanoscale structures, these theories must be modified before using because of the small size effect. Among the suitable continuum theories for nanostructures, we can refer to Eringen's nonlocal, modified couple stress, gradient strain, and surface elasticity theories. The nonlocal theory was adopted by Eringen (Eringen and Edelen 1972) and it is one of the most used continuum theories. Several studies are conducted for vibration, buckling, and bending analysis of the elements, such as plates and beams in micro and nanoscale (Berrabah *et al.* 2013, Reddy 2007, Reddy and Pang 2008, Azrar *et al.* 2016, Żur *et al.* 2020, Akbas 2018, Berghouti *et al.* 2019) under the effect of the several parameters such as temperature, magnetic, crack, and elastic medium(Demir and Civalek 2017, Loya *et al.* 2009, Ma'en 2017, Fazelzadeh and Pouresmaeeli 2013, Hussein *et al.* 2020, Ebrahimi and Mahmoodi 2018, Ebrahimi *et al.* 2019, Abdullah *et al.* 2020a) using the different continuum theories (Apuzzo *et al.* 2017, Donà *et al.*2015, Polizzotto 2014, 2015, 2016, Akbaş 2017, Khorshidi and Shariati 2016). Axial and torsional vibration analyses of nanorods have been investigated in several studies. Barretta *et al.* (2019) used the stress-driven integral elasticity to study the axial vibration of nanorods. Using the nonlocal finite element model, Numanoğlu and Civalek (2019) investigated the effect of the surrounded elastic matrix on the torsional frequencies.

Nonlinear vibration analysis is of importance because most of the vibrating systems approach nonlinear vibration, but for the sake of simplicity, these systems are considered to vibrate linearly. Abdullah et al. investigated (Abdullah *et al.* 2020b) the nonlinear vibration of the embedded single-wall carbon nanotubes (SWCNTs) under the effect of temperature changes and magnetic load. Duc (Duc 2016) conducted the nonlinear thermal vibration of a functionally graded material (FGM) shell using Reddy's third-order shear deformation shell theory. Şimşek (2016) studied the nonlinear vibration of FGM nanobeams using the nonlocal strain gradient theory. Hashemi *et al.* (2015) considered the surface effects to investigate the nonlinear vibration of

*Corresponding author, Ph.D.,
E-mail: rnazemnezhad@du.ac.ir
**Co-corresponding author, Ph.D.,
E-mail: shh@iust.ac.ir
[a] Ph.D.: nazhad.hussein@su.edu.krd
[b] Ph.D., Student: sardar_abd2000@yahoo.com

ISSN: 2287-237X (Print), 2287-2388 (Online)

nanobeams using the nonlocal theory.

As much as the nonlinear vertical vibration of the nanobeams is important, the nonlinear axial and torsional vibrations of plates, bars, and rods in macro, micro, and nanoscale are of importance. Akgoz and Civalek (2011) analyzed the nonlinear vibration of the laminated plates located on the nonlinear elastic foundations. Nazemnezhad *et al*. (2019) investigated the influence of the surface energy on the nonlinear axial vibration of nanorods.

Investigating the nonlinear torsional vibration of the nanorods using different continuum theories such as the nonlocal theory and modified couple stress theory is conducted by Shakhlavi *et al.* (2020) and Setoodeh *et al*. (2016), respectively.

Cracks can affect the torsional vibration characteristics such as the torsional natural frequencies and torsional response of nanorods and nanobeams. Loya *et al.* (2014) examined the crack effects on the torsional frequencies of a nonlocal nanorod model. Studying the effect of the crack on the torsional vibration of carbon nanotubes (CNTs) with torsional restraints using the nonlocal differential model was performed by Yayli *et al*. (2019). Rahmani *et al*. (2015) presented an analytical study to show the crack and boundary condition effects on the torsional vibration on nanobeams. Nazemnezhad and Fahimi (2017) studied the torsional vibration of nanobeams under crack and surface energy effects. Recently, the torsional vibration of the CNTs has been investigated by Abdullah *et al*. (2020c) under the effect of the temperature changes and in the presence of an elastic medium using the Rayleigh-Ritz numerical method. The results of this numerical method well agreed with the compared results of the other results.

Based on the mentioned studies, an absence of an investigation about the thermal stress effects on the torsional vibration of cracked and non-cracked nanorods is obvious. For this reason, this paper investigates the effect of the crack parameters (crack position, crack severity, and crack numbers), elastic medium, length of nanorods, and the nonlocal coefficient on the torsional frequencies in the presence of the three-dimensional thermal stresses. Using nonlinear Green's strains, we expose the effect of the thermal strains and stresses to the equation of motion.

2. Theory

2.1 Materials

The well-known nonlocal elasticity theory is used to expose the small size effect of the nanorods to the equations. The nonlocal theory is generally written into two forms. The first one is the integral form and the second one is the equivalent differential constitutive form which is given by

$$[1-(e_o a)^2\nabla^2]\sigma_{ij} = C_{ijkl}\varepsilon_{kl}(x) = t_{ij} \tag{1}$$

where t_{ij}, σ_{ij}, ε_{ij}, and C_{ijkl} denote the local stress tensor, nonlocal stress tensor, strain tensor, and the component of elasticity tensor, respectively. e_o, a, and $e_o a$ are the nonlocal parameter, characteristic internal length, and nonlocal scale coefficient, respectively.

2.1 Governing equation of motion for CNTs

Three-dimensional displacements of a nanorod are assumed to be as following

$$u = 0 \qquad \mathrm{v} = -z\theta(x,t) \qquad w = y\theta(x,t) \tag{2}$$

Here, u, v, and w are the displacements of the nanorod along x, y, and z axes, respectively. The twist of the cross-section about the x-axis is denoted by angle θ. Eq. (3) shows Green's strain relation

$$\varepsilon_{ij} = \frac{1}{2}\left(\frac{\partial u_i}{\partial x_j} + \frac{\partial u_j}{\partial x_i} + \frac{\partial u_k}{\partial x_i}\frac{\partial u_k}{\partial x_j}\right) \tag{3}$$

Using Eqs. (2) and (3), the mechanical strain components for the nanorod are obtained as

$$\begin{gathered}\varepsilon_{xx} = \frac{1}{2}(y^2+z^2)\left(\frac{\partial\theta}{\partial x}\right)^2 = \frac{1}{2}r^2\left(\frac{\partial\theta}{\partial x}\right)^2 \\ \varepsilon_{yy} = \varepsilon_{zz} = \frac{1}{2}\theta^2 \\ \varepsilon_{xy} = \varepsilon_{yx} = \frac{1}{2}\left(y\theta\frac{\partial\theta}{\partial x} - z\frac{\partial\theta}{\partial x}\right) \\ \varepsilon_{zx} = \varepsilon_{xz} = \frac{1}{2}\left(y\frac{\partial\theta}{\partial x} + z\theta\frac{\partial\theta}{\partial x}\right) \\ \varepsilon_{yz} = \varepsilon_{zy} = 0\end{gathered} \tag{4}$$

In this paper, the nanorods are assumed to be made of carbon nanotubes. Generally, the SWCNTs are anisotropic materials (transversely isotropic) but for the sake of simplicity, they are assumed to be isotropic materials. In this study, the CNTs are assumed to be the same as they are in fact. For the SWCNTs, there are five independent elastic constants which are C_{11}, $C_{22}=C_{33}$, $C_{12}=C_{13}$, C_{23}, and $C_{66}=C_{55}$. These constants can be obtained theoretically, numerically, and experimentally. The corresponding stresses of the SWCNTs are given as following (note that $C_{ij}=C_{ji}$)

$$\begin{gathered}\sigma_{xx} = C_{11}\varepsilon_{xx} + C_{12}\varepsilon_{yy} + C_{13}\varepsilon_{zz} \\ = \frac{1}{2}r^2C_{11}\left(\frac{\partial\theta}{\partial x}\right)^2 + C_{12}\theta^2 \\ \sigma_{yy} = C_{21}\varepsilon_{xx} + C_{22}\varepsilon_{yy} + C_{23}\varepsilon_{zz} \\ = \frac{1}{2}r^2C_{12}\left(\frac{\partial\theta}{\partial x}\right)^2 + \frac{1}{2}(C_{22}+C_{23})\theta^2 \\ \sigma_{zz} = C_{31}\varepsilon_{xx} + C_{32}\varepsilon_{yy} + C_{33}\varepsilon_{zz} \\ = \frac{1}{2}r^2C_{12}\left(\frac{\partial\theta}{\partial x}\right)^2 + \frac{1}{2}(C_{22}+C_{23})\theta^2\end{gathered} \tag{5}$$

$$\sigma_{xy} = 2C_{66}\varepsilon_{xy} = G\gamma_{xy} = G\left(y\theta\frac{\partial\theta}{\partial x} - z\frac{\partial\theta}{\partial x}\right)$$

$$\sigma_{xz} = 2C_{66}\varepsilon_{xz} = G\gamma_{xz} = G\left(y\frac{\partial\theta}{\partial x} + z\theta\frac{\partial\theta}{\partial x}\right)$$

$$\sigma_{yz} = 0$$

The presence of an elastic medium around the SWCNT/nanorod influences the torsional characteristics by inducing the damping and elastic effects. The damping effect of the elastic medium is neglected in the present work. The surrounding elastic medium is modeled as the torsional springs around the SWCNT /nanorod with the torsional stiffness per unit length of K_t. As it is seen from

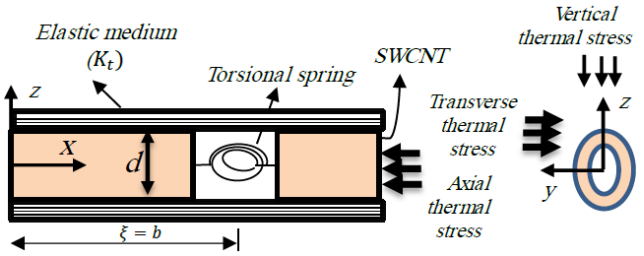

Fig. 1 An embedded cracked nanorod/SWCNT under thermal stresses

Fig. 1, the SWCNT/nanorod with diameter d is exposed to a three-dimensional thermal environment leading to the thermal stresses in axial, transverse (widthwise), and vertical directions.

Mechanical and thermal stresses of the anisotropic SWCNTs are related to the mechanical and thermal strains using the stiffness matrix $[C_{ij}]$ according to Eq. (6) in which σ_{ij}^{Th} are thermal stress components.

$$\begin{Bmatrix} \sigma_{xx}+\sigma_{xx}^{Th} \\ \sigma_{yy}+\sigma_{yy}^{Th} \\ \sigma_{zz}+\sigma_{zz}^{Th} \\ \sigma_{yz}+\sigma_{yz}^{Th} \\ \sigma_{xy}+\sigma_{xy}^{Th} \\ \sigma_{zx}+\sigma_{zx}^{Th} \end{Bmatrix} = \begin{bmatrix} C_{11} & C_{12} & C_{12} & 0 & 0 & 0 \\ C_{12} & C_{22} & C_{23} & 0 & 0 & 0 \\ C_{12} & C_{23} & C_{22} & 0 & 0 & 0 \\ 0 & 0 & 0 & C_{44} & 0 & 0 \\ 0 & 0 & 0 & 0 & C_{66} & 0 \\ 0 & 0 & 0 & 0 & 0 & C_{66} \end{bmatrix} \begin{Bmatrix} \varepsilon_{xx}-\alpha_{xx}\Delta T \\ \varepsilon_{yy}-\alpha_{yy}\Delta T \\ \varepsilon_{zz}-\alpha_{zz}\Delta T \\ 2\varepsilon_{yz} \\ 2\varepsilon_{xy} \\ 2\varepsilon_{zx} \end{Bmatrix} \quad (6)$$

It is worth mentioning that the thermal stresses are normal, and they do not lead to any shear stresses and any resulting torque, thus, $\sigma_{yz}^{Th}=\sigma_{xy}^{Th}=\sigma_{zx}^{Th}=0$.

$$\begin{aligned} \sigma_{xx}^{Th} &= -\left(C_{11}\alpha_{xx}\Delta T + C_{12}\alpha_{yy}\Delta T + C_{13}\alpha_{yy}\Delta T\right) \\ \sigma_{yy}^{Th} &= -\left(C_{12}\alpha_{xx}\Delta T + C_{22}\alpha_{yy}\Delta T + C_{23}\alpha_{yy}\Delta T\right) \\ \sigma_{zz}^{Th} &= -\left(C_{12}\alpha_{xx}\Delta T + C_{23}\alpha_{yy}\Delta T + C_{22}\alpha_{yy}\Delta T\right) \end{aligned} \quad (7)$$

$$\sigma_{ij}^{Th}=0 \quad For\ i\neq j; \quad \alpha_{yy}=\alpha_{zz};$$

$$\Delta T = T - T_{reference}$$

Expressions α_{xx}, α_{yy}, and α_{zz} are the coefficients of thermal expansion in x, y, and z directions. Changes in the temperature is denoted by ΔT in which the stress-free temperature ($T_{reference}$) is set to be equal to the room temperature. For the present study, room temperature is set at 23°C or 296 K.

The surrounding elastic medium causes a torque per unit length of T_E which is given as follows

$$T_E = K_t\theta \quad (8)$$

To obtain the equation of motion and boundary conditions, Hamilton's principle is expressed as follows

$$\delta\int_{t_1}^{t_2}(-T-\mathrm{W}+U_s+U_{Th})\ dt=0 \quad (9)$$

where T, W, U_s, and U_{Th} are the kinetic energy, work done by external torques, strain energy, and potential energy caused by the thermal stresses.

Variations of the T, W, and U_s are determined as

$$\begin{aligned} \delta T &= \delta\int_V \frac{\rho}{2}\left[\left(\frac{\partial u}{\partial t}\right)^2+\left(\frac{\partial v}{\partial t}\right)^2+\left(\frac{\partial w}{\partial t}\right)^2\right] dV \\ &= \int_0^L\int_{\mathrm{Ri}}^{Ro} 2\pi\rho\, r^3 dr\frac{\partial^2\theta}{\partial t^2}dx \\ &= -\int_0^L \mathrm{S}\frac{\partial^2\theta}{\partial t^2}\delta\theta\ dx \end{aligned} \quad (10)$$

$$\delta W = \delta\int_0^L T_{Ext}\,\theta\ dx = \int_0^L T_{Ext}\,\delta\theta\ dx \quad (11)$$

$$\begin{aligned} \delta U_s = \delta\int_V & \frac{1}{2}\left(\sigma_{xx}\varepsilon_{xx}+\sigma_{yy}\varepsilon_{yy}+\sigma_{zz}\varepsilon_{zz}\right. \\ & \left.+\sigma_{xy}\gamma_{xy}+\sigma_{xz}\gamma_{xz}\right) dV \\ = \int_{\mathrm{Ri}}^{Ro} dA & \left\{ \int_0^L \begin{bmatrix} \frac{-3}{2}r^4C_{11}\left(\frac{\partial\theta}{\partial x}\right)^2\frac{\partial^2\theta}{\partial x^2} \\ -r^2C_{12}\theta\left(\frac{\partial\theta}{\partial x}\right)^2-r^2C_{12}\theta^2\frac{\partial^2\theta}{\partial x^2} \\ +(C_{22}+C_{23})\theta^3-Gr^2\frac{\partial^2\theta}{\partial x^2} \\ -Gr^2\theta\left(\frac{\partial\theta}{\partial x}\right)^2-Gr^2\theta^2\frac{\partial^2\theta}{\partial x^2} \end{bmatrix}\delta\theta\, dx \right. \\ & \left. + \left[\begin{pmatrix} \frac{1}{2}r^4C_{11}\left(\frac{\partial\theta}{\partial x}\right)^3+r^2C_{12}\theta^2\frac{\partial\theta}{\partial x} \\ +Gr^2\frac{\partial\theta}{\partial x}+Gr^2\theta^2\frac{\partial\theta}{\partial x} \end{pmatrix}\delta\theta\right]_0^L \right\} \end{aligned} \quad (12)$$

Variation of the potential caused by the thermal stresses δU_{Th} according to Praveen and Reddy (1998) is obtained as

$$\begin{aligned} \delta U_{Th} &= \int_V \left(\sigma_{xx}^{Th}\delta\varepsilon_{xx}+\sigma_{yy}^{Th}\delta\varepsilon_{yy}+\sigma_{zz}^{Th}\delta\varepsilon_{zz}\right) dV \\ &= \left[\left(Q_{xx}^T\frac{\partial\theta}{\partial x}\right)\delta\theta\right]_0^L+\int_0^L\begin{bmatrix} -Q_{xx}^T\frac{\partial^2\theta}{\partial x^2} \\ +(Q_{yy}^T+Q_{zz}^T)\theta \end{bmatrix}\delta\theta\, dx \end{aligned} \quad (13)$$

By substituting Eqs. (10) - (13) into Eq. (9), we arrive at Eq. (20) which includes the equation of motion and boundary conditions

$$\begin{aligned} & \int_{t_1}^{t_2}\int_0^L \begin{bmatrix} -3Q_1\left(\frac{\partial\theta}{\partial x}\right)^2\frac{\partial^2\theta}{\partial x^2}+(-Q_2-Q_4)\theta\left(\frac{\partial\theta}{\partial x}\right)^2 \\ +(-Q_2-Q_4)\theta^2\frac{\partial^2\theta}{\partial x^2}+Q_3\theta^3 \\ +S\frac{\partial^2\theta}{\partial t^2}-Q_4\frac{\partial^2\theta}{\partial x^2}-Q_{xx}^T\frac{\partial^2\theta}{\partial x^2} \\ +(Q_{yy}^T+Q_{zz}^T)\theta-T_{ext} \end{bmatrix}\delta\theta\, dx\, dt \\ & + \int_{t_1}^{t_2}\left[\begin{pmatrix} Q_1\left(\frac{\partial\theta}{\partial x}\right)^3+(Q_2+Q_4)\theta^2\frac{\partial\theta}{\partial x} \\ +(Q_4+Q_{xx}^T)\frac{\partial\theta}{\partial x} \end{pmatrix}\delta\theta\right]_0^L dt=0 \end{aligned} \quad (14)$$

$$\begin{aligned} &\int_{\mathrm{Ri}}^{Ro} dA=\int_{\mathrm{Ri}}^{Ro}2\pi r\, dr;\ I_P=\frac{\pi}{2}(R_o^4-R_i^4); \\ &Q_1=\int_{\mathrm{Ri}}^{Ro}\frac{r^4}{2}C_{11}dA=\frac{\pi}{6}C_{11}(R_o^6-R_i^6); \\ &Q_2=\int_{\mathrm{Ri}}^{Ro}r^2C_{12}dA=C_{12}I_P; \end{aligned} \quad (15)$$

$$Q_3 = \int_{\mathrm{Ri}}^{Ro} (C_{22} + C_{23}) dA = (C_{22} + C_{23}) A;$$
$$Q_4 = \int_{\mathrm{Ri}}^{Ro} G r^2 dA = G I_P;\ S = \int_{\mathrm{Ri}}^{Ro} 2\pi\rho\, r^3 dr = \rho I_P;$$
$$Q_{xx}^T = \int_{\mathrm{Ri}}^{Ro} r^2 \sigma_{xx}^{Th}\, dA = \sigma_{xx}^{Th}\, I_P;$$
$$Q_{yy}^T = \int_{\mathrm{Ri}}^{Ro} \sigma_{yy}^{Th}\, dA = \sigma_{yy}^{Th} A;$$
$$Q_{zz}^T = \int_{\mathrm{Ri}}^{Ro} \sigma_{zz}^{Th}\, dA = \sigma_{zz}^{Th} A;\ T_{Ext} = -T_E = -K_t \theta$$

Here, T_{Ext} is the total external torque per unit length and ρ is the density. From Eq. (14), the equation of motion is as

$$\begin{aligned} &-3Q_1 \left(\frac{\partial\theta}{\partial x}\right)^2 \frac{\partial^2\theta}{\partial x^2} + (-Q_2 - Q_4)\theta \left(\frac{\partial\theta}{\partial x}\right)^2 \\ &+(-Q_2 - Q_4)\theta^2 \frac{\partial^2\theta}{\partial x^2} + Q_3\theta^3 + S\frac{\partial^2\theta}{\partial t^2} - Q_4 \frac{\partial^2\theta}{\partial x^2} \\ &-Q_{xx}^T \frac{\partial^2\theta}{\partial x^2} + \left(Q_{yy}^T + Q_{zz}^T\right)\theta - T_{Ext} = 0 \end{aligned} \tag{16}$$

Let's rewrite the differential nonlocal equation shown in Eq. (1) in the presence of the thermal stresses as

$$\begin{aligned} [1 - (e_o a)^2 \nabla^2]\sigma_{ij} &= C_{ijkl}\varepsilon_{kl} - C_{ijkl}\alpha_{kl}\Delta T \\ &= C_{ijkl}\varepsilon_{kl} + \sigma_{ij}^{Th} \end{aligned} \tag{17}$$

To obtain the nonlocal equation of motion, the following relations are used

$$[1 - (e_o a)^2 \nabla^2]\sigma_{xx} = C_{11}\varepsilon_{xx} + C_{12}\varepsilon_{yy} + C_{13}\varepsilon_{zz} + \sigma_{xx}^{Th} \tag{18}$$

$$[1 - (e_o a)^2 \nabla^2]\sigma_{yy} = C_{21}\varepsilon_{xx} + C_{22}\varepsilon_{yy} + C_{23}\varepsilon_{zz} + \sigma_{yy}^{Th} \tag{19}$$

$$[1 - (e_o a)^2 \nabla^2]\sigma_{zz} = C_{31}\varepsilon_{xx} + C_{32}\varepsilon_{yy} + C_{33}\varepsilon_{zz} + \sigma_{zz}^{Th} \tag{20}$$

$$[1 - (e_o a)^2 \nabla^2]\sigma_{xy} = G\gamma_{xy} \tag{21}$$

$$[1 - (e_o a)^2 \nabla^2]\sigma_{xz} = G\gamma_{xz} \tag{22}$$

Following equations are obtained from Eqs. (18) to (22) in which the superscript "nl" means nonlocal

$$\begin{aligned} &[1 - (e_o a)^2 \nabla^2]P_{x1}^{nl} = P_{x1}; \\ &[1 - (e_o a)^2 \nabla^2]P_{x2}^{nl} = P_{x2}; \\ &[1 - (e_o a)^2 \nabla^2]P_{x3}^{nl} = P_{x3} \end{aligned} \tag{23}$$

$$\begin{aligned} &[1 - (e_o a)^2 \nabla^2]P_{y1}^{nl} = P_{y1}; \\ &[1 - (e_o a)^2 \nabla^2]P_{y2}^{nl} = P_{y2}; \\ &[1 - (e_o a)^2 \nabla^2]P_{y3}^{nl} = P_{y3} \end{aligned} \tag{24}$$

$$\begin{aligned} &[1 - (e_o a)^2 \nabla^2]P_{z1}^{nl} = P_{z1}; \\ &[1 - (e_o a)^2 \nabla^2]P_{z2}^{nl} = P_{z2}; \\ &[1 - (e_o a)^2 \nabla^2]P_{z3}^{nl} = P_{z3} \end{aligned} \tag{25}$$

$$[1 - (e_o a)^2 \nabla^2]P_{xy}^{nl} = P_{xy} \tag{26}$$

$$[1 - (e_o a)^2 \nabla^2]P_{xz}^{nl} = P_{xz} \tag{27}$$

$$\begin{aligned} &\int r^2(\sigma_{xx} + \sigma_{xx}^{Th})dA = P_{x1} + P_{x2} + P_{x3}; \\ &\int \left(\sigma_{yy} + \sigma_{yy}^{Th}\right)dA = P_{y1} + P_{y2} + P_{y3}; \\ &\int (\sigma_{zz} + \sigma_{zz}^{Th})dA = P_{z1} + P_{z2} + P_{z3}; \\ &\int \sigma_{xy}\gamma_{xy} dA = P_{xy}; \quad \int \sigma_{xz}\gamma_{xz} dA = P_{xz}; \\ &P_{x1} = Q_1 \left(\frac{\partial\theta}{\partial x}\right)^2; \quad P_{x2} = Q_2\theta^2; \quad P_{x3} = Q_{xx}^T; \\ &P_{y1} = P_{z1} = \frac{Q_2}{2}\left(\frac{\partial\theta}{\partial x}\right)^2; \quad P_{y2} = P_{z2} = \frac{Q_3}{2}\theta^2; \\ &P_{y3} = Q_{yy}^T; \quad P_{z3} = Q_{zz}^T. \end{aligned} \tag{28}$$

To obtain the nonlocal form of the equation of motion shown in Eq. (16), we use the expressions of Eq. (28) as

$$\begin{aligned} &-3P_{x1}\frac{\partial^2\theta}{\partial x^2} + \left(-P_{y1} - P_{z1}\right)\theta - \frac{\partial P_{xy}}{\partial x}\frac{1}{2\left(\frac{\partial\theta}{\partial x}\right)} \\ &-\frac{\partial P_{xz}}{\partial x}\frac{1}{2\left(\frac{\partial\theta}{\partial x}\right)} - P_{x2}\frac{\partial^2\theta}{\partial x^2} + \left(P_{y2} + P_{z2}\right)\theta - P_{x3}\frac{\partial^2\theta}{\partial x^2} \\ &+\left(P_{y3} + P_{z3}\right)\theta + S\frac{\partial^2\theta}{\partial t^2} - T_{Ext} = 0 \end{aligned} \tag{29}$$

The nonlocal equation of motion is obtained by replacing Eqs. (23) - (27) into Eq. (29)

$$\begin{aligned} &-3[1 - (e_o a)^2 \nabla^2]P_{x1}^{nl}\frac{\partial^2\theta}{\partial x^2} - [1 - (e_o a)^2 \nabla^2]P_{y1}^{nl}\theta - \\ &[1 - (e_o a)^2 \nabla^2]P_{z1}^{nl}\theta - \frac{\partial[1 - (e_o a)^2 \nabla^2]P_{xy}^{nl}}{\partial x}\frac{1}{2\left(\frac{\partial\theta}{\partial x}\right)} \\ &-\frac{\partial[1 - (e_o a)^2 \nabla^2]P_{xz}^{nl}}{\partial x}\frac{1}{2\left(\frac{\partial\theta}{\partial x}\right)} - [1 - (e_o a)^2 \nabla^2]P_{x2}^{nl}\frac{\partial^2\theta}{\partial x^2} \\ &+[1 - (e_o a)^2 \nabla^2]P_{y2}^{nl}\theta + [1 - (e_o a)^2 \nabla^2]P_{z2}^{nl}\theta \\ &-[1 - (e_o a)^2 \nabla^2]P_{x3}^{nl}\frac{\partial^2\theta}{\partial x^2} + [1 - (e_o a)^2 \nabla^2]P_{y3}^{nl}\theta \\ &+[1 - (e_o a)^2 \nabla^2]P_{z3}^{nl}\theta + [1 - (e_o a)^2 \nabla^2]S\frac{\partial^2\theta}{\partial t^2} \\ &-[1 - (e_o a)^2 \nabla^2]\, T_{Ext} = 0 \end{aligned} \tag{30}$$

Finally, the nonlocal equation of motion is written in a more convenient form as

$$\begin{aligned} &-3Q_1 \left(\frac{\partial\theta}{\partial x}\right)^2 \frac{\partial^2\theta}{\partial x^2} + (-Q_2 - Q_4)\theta \left(\frac{\partial\theta}{\partial x}\right)^2 \\ &+(-Q_2 - Q_4)\theta^2 \frac{\partial^2\theta}{\partial x^2} + Q_3\theta^3 + S\frac{\partial^2\theta}{\partial t^2} \\ &-(e_o a)^2 S\frac{\partial^4\theta}{\partial x^2 \partial t^2} - Q_4\frac{\partial^2\theta}{\partial x^2} - Q_{xx}^T\frac{\partial^2\theta}{\partial x^2} \\ &+\left(Q_{yy}^T + Q_{zz}^T\right)\theta - T_{Ext} + (e_o a)^2\frac{\partial^2 T_{Ext}}{\partial x^2} = 0 \end{aligned} \tag{31}$$

Eq. (31) is a nonlinear equation that consists of both linear and nonlinear parts. The present study aims to examine the thermal stresses on the linear torsional frequency in the presence of the crack and elastic medium. For this reason, we can neglect the nonlinear terms of the equation of motion, and finally, we arrive at a linear equation of motion that can be solved both analytically and numerically. The linear equation of motion and its related boundary conditions are obtained as

$$S\frac{\partial^2\theta}{\partial t^2}-(e_oa)^2S\frac{\partial^4\theta}{\partial x^2\,\partial t^2}-Q_4\frac{\partial^2\theta}{\partial x^2}-Q_{xx}^T\frac{\partial^2\theta}{\partial x^2}+\left(Q_{yy}^T+Q_{zz}^T\right)\theta+K_t\theta-(e_oa)^2K_t\frac{\partial^2\theta}{\partial x^2}=0 \quad (32)$$

$$\left[\left(Q_4\frac{\partial\theta}{\partial x}+Q_{xx}^T\frac{\partial\theta}{\partial x}\right)\delta\theta\right]_0^L=0 \quad (33)$$

The separation method is given by Eq. (34) in which ω denotes the nanorod natural frequency

$$\theta(x,t)=\Theta(x)\,e^{i\omega t} \quad (34)$$

Substituting Eq. (34) into Eq. (32) and applying the following dimensionless expressions

$$\xi=x/L;\quad \Theta(x)=\bar{\Theta}(\xi);\quad h=e_oa/L;\quad \lambda^2=\frac{S\,L^2}{Q_4}\omega^2;\quad \bar{N}_x^T=\frac{Q_{xx}^T}{Q_4};\quad \bar{N}_y^T=\frac{Q_{yy}^T\,L^2}{Q_4};\quad \bar{N}_z^T=\frac{Q_{zz}^T\,L^2}{Q_4};\quad \bar{K}=\frac{K_t\,L^2}{Q_4}, \quad (35)$$

we arrive at the motion equation in dimensionless form as

$$(-1+h^2\lambda^2-h^2\bar{K}-\bar{N}_x^T)\frac{d^2\bar{\Theta}(\xi)}{d\xi^2}+\left(\bar{N}_y^T+\bar{N}_z^T+\bar{K}-\lambda^2\right)\bar{\Theta}(\xi)=0 \quad (36)$$

$$\frac{d^2\bar{\Theta}(\xi)}{d\xi^2}+\frac{\left(\lambda^2-\bar{N}_y^T-\bar{N}_z^T-\bar{K}\right)}{(1-h^2\lambda^2+h^2\bar{K}+\bar{N}_x^T)}\bar{\Theta}(\xi)=0 \quad (37)$$

$$\frac{d^2\bar{\Theta}(\xi)}{d\xi^2}+\Lambda^2\bar{\Theta}(\xi)=0 \quad (38)$$

$$\Lambda^2=\frac{\left(\lambda^2-\bar{N}_y^T-\bar{N}_z^T-\bar{K}\right)}{(1-h^2\lambda^2+h^2\bar{K}+\bar{N}_x^T)}\;\rightarrow\;\lambda^2=\frac{\Lambda^2(1+h^2\bar{K}+\bar{N}_x^T)+\bar{N}_y^T+\bar{N}_z^T+\bar{K}}{(1+\Lambda^2h^2)} \quad (39)$$

Substituting $\bar{\Theta}(\xi)=De^{S\xi}$ into Eq. (38), we obtain the roots of Eq. (38) as follows

$$S_1=i\Lambda\qquad S_2=-i\Lambda \quad (40)$$

The general solution of Eq. (38) is obtained as

$$\bar{\Theta}(\xi)=A_1\sin(\Lambda\xi)+A_2\cos(\Lambda\xi) \quad (41)$$

2.2 Cracked nanorod equations

It is assumed that the nanorod has a defect such as a crack at a dimensionless distance from the nanorod left end of $b=L_c/L$ (L_c is the distance from the nanorod left end). The crack can be modeled as a torsional spring which induces more flexibility to the nanorod and it divides the nanorod into two segments (see Fig. 1). Each nanorod segment has its equation of motion. Eq. (42) is used for the cracked nanorods in which "n" is the number of the cracks and "i" is the number of the nanorod segments. For the single-cracked and double-cracked nanorods, we obtain two and three equations from Eq. (42), respectively. The crack severity is denoted by C_s which is the flexibility of the equivalent spring representing a torsional crack.

$$\bar{\Theta}_i(\xi)=A_{i1}\sin(\Lambda\xi)+A_{i2}\cos(\Lambda\xi);\quad i=1,2,\ldots.,n+1 \quad (42)$$

The boundary conditions are not sufficient to solve the equations of the cracked nanorods (nontrivial solution). For this reason, the compatibility equations at the crack position are required because each end of the nanorod possesses only one displacement. The compatibility equations at the crack location are as following

Jump in twisting deflection:

$$\Delta\bar{\Theta}=\bar{\Theta}_2(b)-\bar{\Theta}_1(b)=C_s\left.\frac{\partial\bar{\Theta}_1(\xi)}{\partial\xi}\right|_{\xi=b} \quad (43)$$

Continuity of the twisting moment:

$$\left.\frac{\partial\bar{\Theta}_1(\xi)}{\partial\xi}\right|_{\xi=b}=\left.\frac{\partial\bar{\Theta}_2(\xi)}{\partial\xi}\right|_{\xi=b} \quad (44)$$

According to Eq. (33), the boundary conditions for the fixed and free nanorod ends are

$$\text{Fixed end:}\quad \bar{\Theta}(\xi)=0;\quad \text{Free end:}\quad \frac{\partial\bar{\Theta}(\xi)}{\partial\xi}=0 \quad (45)$$

3. Results and discussions

3.1 Validation study

A comparison study is conducted to check the accuracy of the present study results. The comparison of the results of the present study with the results of the indicated references in Table 1 verifies that the present study results are reliable.

Table 1 Comparison of the torsional frequencies of cracked C-F nanorod ($K_t=e_oa=\Delta T=0$ and $b=0.5$)

	$C_s=0$			$C_s=0.05$			$C_s=0.35$		
	λ_1	λ_2	λ_3	λ_1	λ_2	λ_3	λ_1	λ_2	λ_3
Present	1.5708	4.7124	7.8540	1.5325	4.5979	7.6647	1.3404	4.0910	6.9699
Ref 1*	1.570	4.712	7.853	1.532	4.597	7.664	1.340	4.091	6.969
Ref 2*	1.57	4.7	7.82	1.53	4.60	7.64	1.34	4.08	6.97

1* (Nazemnezhad *et al.* 2017)
2* (Loya *et al.* 2014)

Table 2 Properties and geometrical characteristics of a SWCNT of chirality (5,5)

$\rho\ (kg/m^3)$	$d(nm)$	$t(nm)$	$E_{xx}\ (TPa)$	$\nu_{xy}=\nu_{xz}$	At high temperatures	
					$\alpha_{xx}\ (1/K)$	$\alpha_{yy}\ (1/K)$
2300	0.678	0.34	0.968	0.285	1.1×10^{-6}	0.8×10^{-6}
	Elastic constants				At low temperatures	
$C_{11}(TPa)$	$C_{12}(TPa)$	$C_{22}(TPa)$	$C_{44}(TPa)$	$C_{66}(TPa)$	$\alpha_{xx}\ (1/K)$	$\alpha_{yy}\ (1/K)$
1.0528	0.1487	0.3952	0.1347	0.434	-1.6×10^{-6}	-0.5×10^{-6}

Table 3 First three dimensionless torsional frequencies of a cracked C-C nanorod with different crack severities (C_s) for different temperature changes without the elastic medium ($K_t=0,\ L=20\,nm,\ e_oa=2\,nm$, and $b=0.25$)

C_s	Room temperature or higher (ΔT)				Room temperature or lower (ΔT)			
	$\Delta T\ (K)$	λ_1	λ_2	λ_3	$\Delta T\ (K)$	λ_1	λ_2	λ_3
0	0	2.9972	5.3202	6.8587	0	2.9972	5.3202	6.8587
	40	2.9517	5.2998	6.8468	40	3.0358	5.3377	6.8691
	120	2.8585	5.2589	6.8230	120	3.1116	5.3727	6.8898
	300	2.6368	5.1657	6.7690	200	3.1856	5.4074	6.9105
0.15	0	2.8253	5.3202	6.5380	0	2.8253	5.3202	6.5380
	40	2.7765	5.2998	6.5245	40	2.8667	5.3377	6.5496
	120	2.6762	5.2589	6.4977	120	2.9476	5.3727	6.5729
	300	2.4354	5.1657	6.4368	200	3.0264	5.4074	6.5961
0.35	0	2.6701	5.3202	6.1900	0	2.6701	5.3202	6.1900
	40	2.6179	5.2998	6.1748	40	2.7142	5.3377	6.2032
	120	2.5103	5.2589	6.1444	120	2.8003	5.3727	6.2294
	300	2.2494	5.1657	6.0753	200	2.8838	5.4074	6.2556
0.65	0	2.5247	5.3202	5.9092	0	2.5247	5.3202	5.9092
	40	2.4690	5.2998	5.8925	40	2.5716	5.3377	5.9237
	120	2.3537	5.2589	5.8589	120	2.6630	5.3727	5.9525
	300	2.0709	5.1657	5.7827	200	2.7514	5.4074	5.9813
0.95	0	2.4339	5.3202	5.7619	0	2.4339	5.3202	5.7619
	40	2.3758	5.2998	5.7443	40	2.4827	5.3377	5.7771
	120	2.2551	5.2589	5.7090	120	2.5777	5.3727	5.8074
	300	1.9567	5.1657	5.6288	200	2.6693	5.4074	5.8375

Table 4 First three dimensionless torsional frequencies of a cracked C-F nanorod with different crack severities (C_s) for different temperature changes without the elastic medium ($K_t=0,\ L=20\,nm,\ e_oa=2\,nm$, and $b=0.25$)

C_s	Room temperature or higher (ΔT)				Room temperature or lower (ΔT)			
	$\Delta T\ (K)$	λ_1	λ_2	λ_3	$\Delta T\ (K)$	λ_1	λ_2	λ_3
0	0	1.5518	4.2628	6.1767	0	1.5518	4.2628	6.1767
	40	1.4556	4.2340	6.1614	40	1.6299	4.2875	6.1899
	120	1.2410	4.1758	6.1308	120	1.7759	4.3365	6.2163
	300	0.4879	4.0418	6.0614	200	1.9108	4.3849	6.2426
0.15	0	1.3855	4.1962	6.0776	0	1.3855	4.1962	6.0776
	40	1.2763	4.1667	6.0619	40	1.4729	4.2214	6.0913
	120	1.0235	4.1072	6.0302	120	1.6337	4.2715	6.1186
	300	…	3.9700	5.9583	200	1.7800	4.3209	6.1458
0.35	0	1.2259	4.1323	5.9279	0	1.2259	4.1323	5.9279

Table 4 Continued

C_s	Room temperature or higher (ΔT)				Room temperature or lower (ΔT)			
	$\Delta T\ (K)$	λ_1	λ_2	λ_3	$\Delta T\ (K)$	λ_1	λ_2	λ_3
0.35	40	1.1005	4.1022	5.9113	40	1.3243	4.1580	5.9423
	120	0.7920	4.0413	5.8779	120	1.5017	4.2091	5.9710
	300	…	3.9009	5.8022	200	1.6603	4.2596	5.9995
0.65	0	1.0626	4.0699	5.7571	0	1.0626	4.0699	5.7571
	40	0.9144	4.0392	5.7395	40	1.1751	4.0962	5.7723
	120	0.5003	3.9770	5.7041	120	1.3726	4.1484	5.8027
	300	…	3.8334	5.6238	200	1.5451	4.1999	5.8329
0.95	0	0.9501	4.0302	5.6532	0	0.9501	4.0302	5.6532
	40	0.7804	3.9990	5.6350	40	1.0746	4.0568	5.6690
	120	0.1479	3.9360	5.5984	120	1.2881	4.1097	5.7004
	300	…	3.7903	5.5151	200	1.4709	4.1619	5.7316

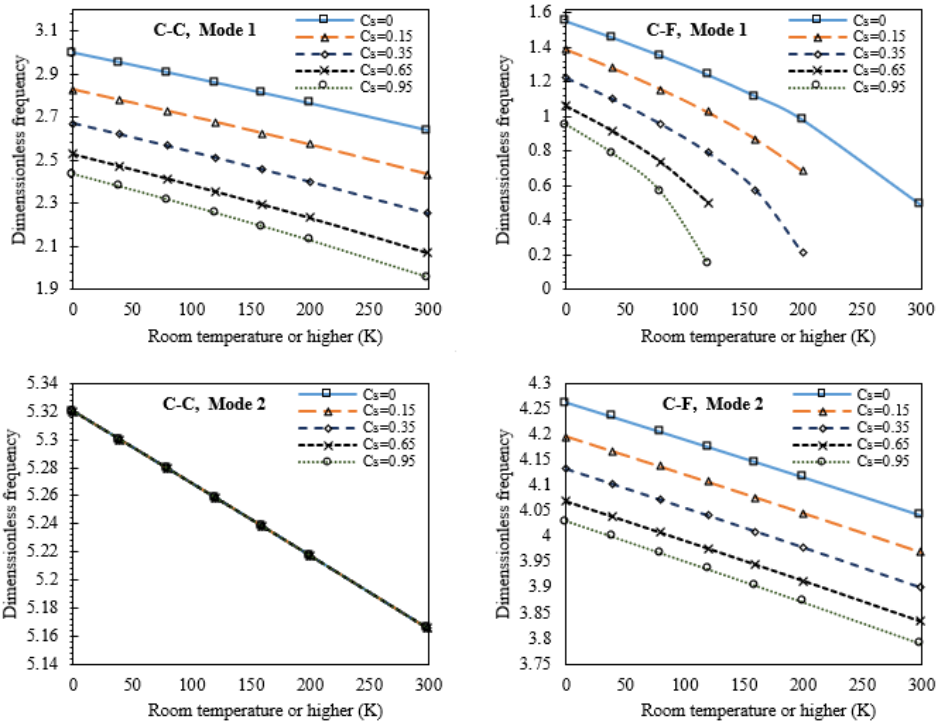

Fig. 2 Variation of first two frequencies of cracked C-C and C-F nanorods with room temperature or higher, for different crack severities ($K_t = 0,\ L = 20\ nm,\ e_o a = 2\ nm$, and $b = 0.25$)

3.2 Benchmark results

In the present study, thermal and mechanical properties, and geometries of the armchair SWCNTs with chirality (5,5) are chosen according to Lu (Lu 1997) and are presented in Table 2. The nanorod length of $L = 20\ nm$ is considered but to examine the nanorod length effect on the frequencies, the different lengths are used within the range 5-25 nm. The values of the thermal expansion coefficients are presented in Table 2, are considered according to Yoa and Han (Yao and Han 2006) for room temperature or lower (low temperature) and for temperatures higher than room temperature (high temperature). Different values are reported for the nonlocal scale coefficient "$e_o a$" but none of them is certain. Thus, a range of 0-2 nm is considered in this study as described by Wang and Wang (Wang and Wang 2007). The cross-section area A can be calculated by Eq. (46) in which the mean, inner, and outermost radiuses of the SWCNT are indicated by R, R_i, and R_o, respectively.

$$A = \pi\left(R_o^2 - R_i^2\right); \quad R = \frac{d}{2}; \quad R_i = R - \frac{t}{2}; \quad R_o = R + \frac{t}{2}; \tag{46}$$

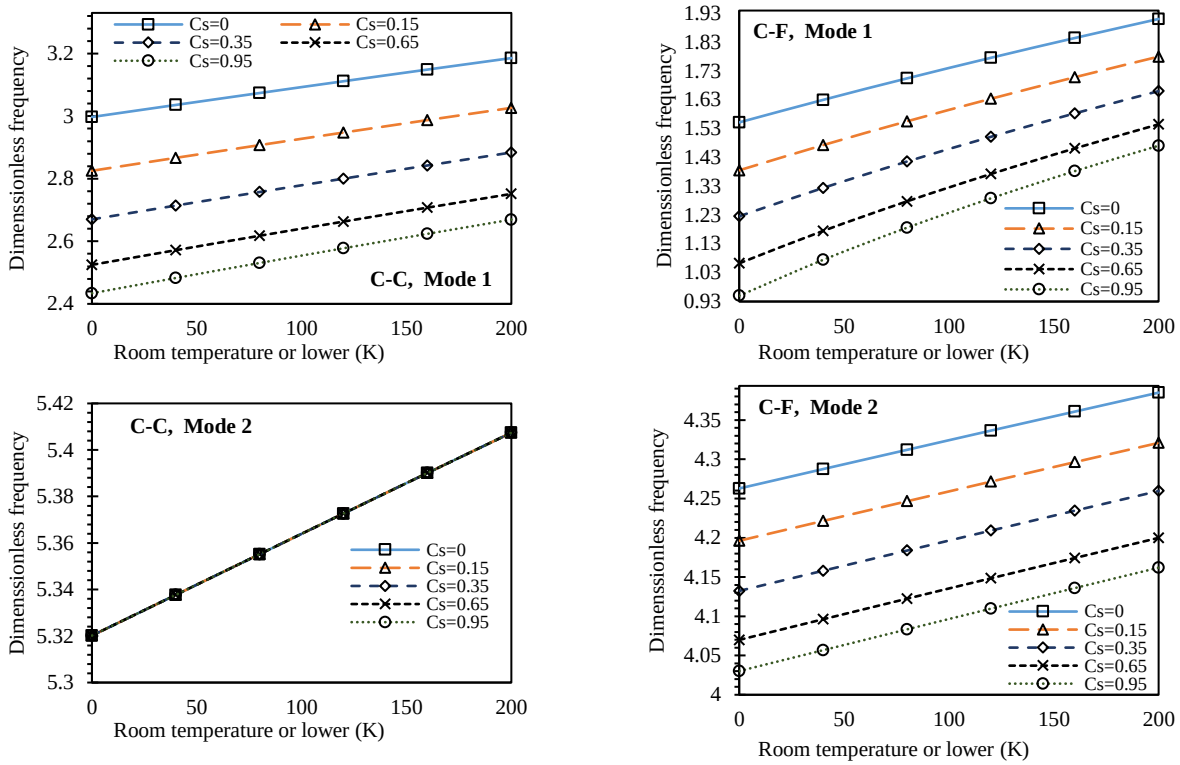

Fig. 3 Variation of first two frequencies of cracked C-C and C-F nanorods with room temperature or lower, for different crack severities ($K_t = 0,\ L = 20\ nm,\ e_o a = 2\ nm$, and $b = 0.25$)

The torsional frequencies of the cracked fixed-fixed (C-C) and fixed-free (C-F) nanorods at room temperature, lower, and higher in the absence of the elastic medium are tabulated in Table 3 and Table 4, respectively. Except for the second mode of the C-C nanorod, other frequencies of the C-C and C-F nanorods decrease with an increase in the crack severity at any temperature for the crack position of $b = 0.25$.

At temperatures higher than room temperature, the frequencies of all modes decrease, and as much as the temperature gets higher, its effect on the torsional frequencies increases for the cracked and non-cracked C-C and C-F rods for any crack severity as shown in Fig. 2. This is because of a reduction in the torsional stiffness of the nanorod as it has been already reported by Mehta and Kumar (Mehta and Kumar 1994) that the torsional characteristics are temperature-dependent. On the contrary, at temperatures lower than room temperature, the frequencies of the cracked and non-cracked C-C and C-F nanorods increase for any crack severity as shown in Fig. 3. The frequencies increase more as the temperature gets lower. The presence of the crack leads to a reduction in the nanorod stiffness and as much as its severity increases, a more reduction in the frequencies is observed at low and high temperatures. For this reason, for the C-F nanorod when values of the high temperature and crack severity increase, the first mode frequency approaches to a minimum value as seen in Fig. 2. This is due to the extraordinary flexibility introduced by both crack and high temperature to the nanorod. The second mode of the C-C nanorod is independent of the crack severity. It means that the presence and absence of the crack do not affect the second mode of this nanorod type at any temperature value. This is because of the symmetry in the boundary condition. Such a phenomenon has already been observed for some of the lateral frequencies of the simply supported and clamped-clamped nanobeams.

The comparative parameter of "difference percent" is a suitable tool to show the net influence of a particular temperature on the torsional frequencies. The value of the difference percent depends on the values of the other parameters such as $C_s,\ b,\ K_t,\ L$, and d.

$$\text{Difference percent} = \frac{100 \times |frequency_{\Delta T=\Delta T} - frequency_{\Delta T=0}|}{frequency_{\Delta T=0}} \quad (47)$$

where $frequency_{\Delta T=0}$ is the frequency at room temperature.

An increase in the crack severity results in an increase in the difference percent of both C-C and C-F nanorods except the second mode of the C-C nanorod as seen from Fig. 4. As the vibration mode increases, the difference percent reduces as it is seen the first mode difference percent is more than the second and the third modes. The effect of the thermal loads in the form of temperature changes is not negligible especially for a cracked nanorod and it must be taken into account during the design of the nanorods and nanoscale structures.

The crack position (location) is another factor that plays

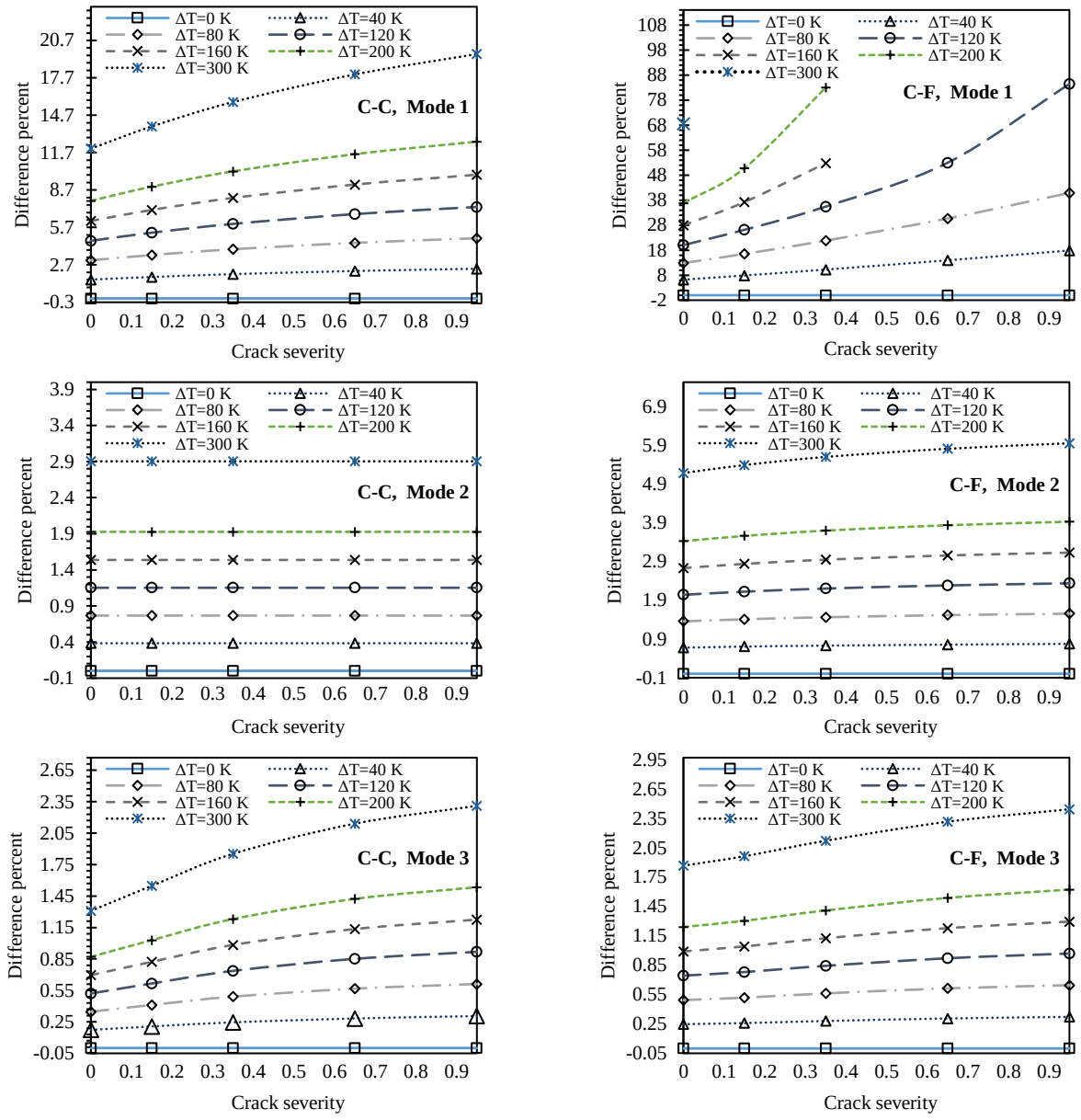

Fig. 4 Difference percent of first three modes of C-C and C-F nanorods with crack severity at room temperature or higher ($K_t = 0,\ L = 20\ nm,\ e_o a = 2\ nm$, and $b = 0.25$)

Table 5 First three dimensionless torsional frequencies of cracked C-C and C-F nanorods with different crack positions (b) for room temperature or higher ($K_t = 0,\ L = 20\ nm,\ e_o a = 2\ nm$, and $C_s = 0.15$)

b	$\Delta T\ (K)$	C-C			C-F		
		λ_1	λ_2	λ_3	λ_1	λ_2	λ_3
0	0	2.6518	4.8766	6.4845	1.3557	3.8370	5.7572
	40	2.5992	4.8531	6.4708	1.2438	3.8037	5.7397
	120	2.4907	4.8057	6.4434	0.9824	3.7362	5.7043
	200	2.3772	4.7579	6.4158	0.6191	3.6675	5.6687
	240	2.3184	4.7337	6.4020	0.3039	3.6326	5.6509
0.05	0	2.6723	4.9609	6.6077	1.3588	3.8884	5.8666
	40	2.6202	4.9380	6.5946	1.2472	3.8557	5.8496
	120	2.5127	4.8919	6.5684	0.9868	3.7894	5.8156
	200	2.4004	4.8454	6.5421	0.6260	3.7219	5.7813

Table 5 Continued

b	$\Delta T\ (K)$	C-C			C-F		
		λ_1	λ_2	λ_3	λ_1	λ_2	λ_3
0.05	240	2.3422	4.8220	6.5289	0.3177	3.6878	5.7641
0.25	0	2.8253	5.3202	6.5380	1.3855	4.1962	6.0776
	40	2.7765	5.2998	6.5245	1.2763	4.1667	6.0619
	120	2.6762	5.2589	6.4977	1.0235	4.1072	6.0302
	200	2.5719	5.2177	6.4707	0.6828	4.0468	5.9984
	240	2.5182	5.1970	6.4571	0.4189	4.0162	5.9824
0.5	0	2.9972	4.8196	6.8587	1.4462	4.0228	5.9225
	40	2.9517	4.7957	6.8468	1.3422	3.9916	5.9058
	120	2.8585	4.7474	6.8230	1.1050	3.9284	5.8724
	200	2.7622	4.6986	6.7990	0.8003	3.8641	5.8388
	240	2.7127	4.6740	6.7870	0.5919	3.8316	5.8219
0.7	0	2.8734	5.2606	6.3957	1.5047	3.8051	5.9631
	40	2.8255	5.2399	6.3816	1.4051	3.7714	5.9467
	120	2.7273	5.1982	6.3533	1.1811	3.7032	5.9137
	200	2.6254	5.1561	6.3248	0.9031	3.6336	5.8806
	240	2.5729	5.1349	6.3106	0.7251	3.5983	5.8639
0.75	0	2.8253	5.3202	6.5380	1.5179	3.8311	5.8212
	40	2.7765	5.2998	6.5245	1.4193	3.7977	5.8040
	120	2.6762	5.2589	6.4977	1.1980	3.7301	5.7694
	200	2.5719	5.2177	6.4707	0.9252	3.6612	5.7346
	240	2.5182	5.1970	6.4571	0.7525	3.6263	5.7171
0.85	0	2.7372	5.1755	6.8472	1.5390	4.0043	5.6805
	40	2.6865	5.1542	6.8352	1.4419	3.9729	5.6625
	120	2.5821	5.1113	6.8113	1.2249	3.9093	5.6262
	200	2.4734	5.0680	6.7873	0.9599	3.8446	5.5897
	240	2.4171	5.0462	6.7752	0.7950	3.8119	5.5714
1	0	2.6518	4.8766	6.4845	1.5518	4.2628	6.1767
	40	2.5992	4.8531	6.4708	1.4556	4.2340	6.1614
	120	2.4907	4.8057	6.4434	1.2410	4.1758	6.1308
	200	2.3772	4.7579	6.4158	0.98051	4.1168	6.1001
	240	2.3184	4.7337	6.4020	0.8198	4.0870	6.0846

an important role in the torsional frequency changes. Table 5 shows the results of some arbitrary crack locations for the C-C and C-F nanorod at room temperature or higher.

The non-cracked nanorods always possess higher frequencies contrasting to the cracked nanorods. Fig. 5 demonstrates that for a C-C rod when the crack locates at the middle of the nanorod ($b = 0.5$), the first mode frequency and frequency ratio are not affected by the crack. But, for the same mode, when the crack locates at the boundary of the nanorods ($b = 0$ and $b = 1$), the torsional frequency and frequency ratio are extremely suppressed by the crack location and the temperature changes as they get their lowest values at high temperatures. It is worth mentioning that for a C-C nanorod the boundaries points ($b = 0$ and $b = 1$) have the same frequencies because of the symmetry in the boundary, but for a C-F nanorod, the frequencies of the crack position of $b = 0$ differ from those of point $b = 1$. However, for the C-F nanorod, the frequencies of the crack location of $b = 1$ equal to those of the non-cracked. Starting from the crack position of $b = 0$, for the C-F nanorod, we observe that the first torsional frequency increases with distancing from the fixed end as shown in Fig. 5. The frequency ratio of the first mode of the C-F nanorod increases by distancing from the fixed end and at the same time, it is less affected by the high temperatures. All torsional frequencies of any boundary condition with or without crack and any crack location (for cracked cases) decrease with an increase in the temperature.

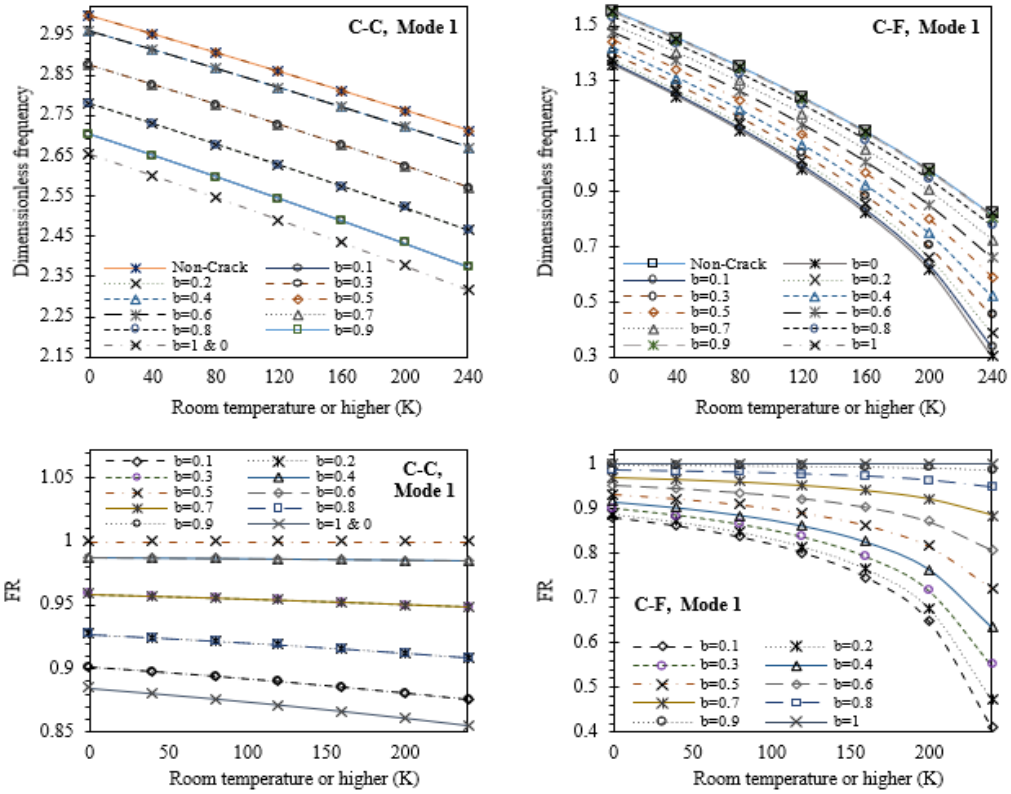

Fig. 5 Frequency and frequency ratio of the first mode of cracked C-C and C-F nanorods at different temperatures and crack positions ($K_t = 0,\ L = 20\ nm,\ e_o a = 2\ nm$, and $C_s = 0.15$)

The effect of the crack position on the difference percent of the C-C and C-F nanorods is shown in Fig. 6. Generally, it is observed that the crack positions in which thefrequencies are highest compared to the other positions have the lowest difference percent and vice versa. It means that the influence of the temperature on the frequencies becomes more at some crack positions. The crack locating at the boundary points of the C-C nanorod leads to the highest difference percent contrasting to the other points. While for a C-C nanorod, the temperature effect (differencepercent) reaches its maximum when the crack locates at a farther distance from the fixed end ($b = 1$). We can recognize in which crack position the difference percent of a certain mode has its maximum and minimum values at a given temperature from Fig. 6. The C-F nanorods are more impressed by the temperature changes comparing to the C-C nanorods for any mode and any crack position.

The torsional frequencies of the cracked C-F nanorod for different values of the nonlocal scale coefficients at different temperatures and crack severities are presented in Table 6. Increasing the nonlocal coefficient causes a decrease in the frequencies of all modes at any temperature and any crack severity. The torsional frequency and difference percent of the cracked C-C and C-F nanorods are shown in Fig. 7. The lowest frequency of the first mode of both C-C and C-F nanorods belongs to the highest nonlocal scale coefficient and crack severity values while the effect of the crack severity on the frequencies is higher than the nonlocal coefficient. The change of the difference percent due to the changes in the nonlocal scale coefficient is approximately zero. This means that the effect of the temperature on the frequencies of the C-C and C-F nanorods is independent of the nonlocal coefficient value.

The presence of the elastic medium increases the torsional frequencies of the non-cracked (i.e., C_s=0) and cracked nanorods according to the results of Table 7. As the stiffness of the elastic medium increases, the frequencies of the non-cracked and cracked C-C and C-F nanorods increase.

According to Fig 8, the highest frequency of the cracked nanorods belongs to the case of the lowest crack severity and the highest elastic medium stiffness for both C-C and C-F. As the temperature increases, the frequency decreases at any value of the elastic medium stiffness, but for the nanorods with a more stiffened elastic medium, the temperature effect decreases. The lowest frequency ratio belongs to the case in which the elastic medium stiffness is the lowest and the crack severity is a high value. An increase in the stiffness of the elastic medium leads to a decrease in the temperature effect on the frequencies for the C-C and C-F nanorods. The amount of the difference percent reduction of the C-F nanorod is higher than the C-C nanorod when the elastic medium is introduced to the nanorod and its stiffness increases.

Another parameter that influences the torsional frequencies is nanorod length. Table 8 shows that when the nanorod lengthens, all mode frequencies increase at any temperature and any crack severity value. Reduction of all frequencies of the nanorods especially the first mode of the C-F nanorod due to the high temperatures approaches a maximum value when the nanorod length increases to a relatively high value. As shown in Fig. 9, increasing the

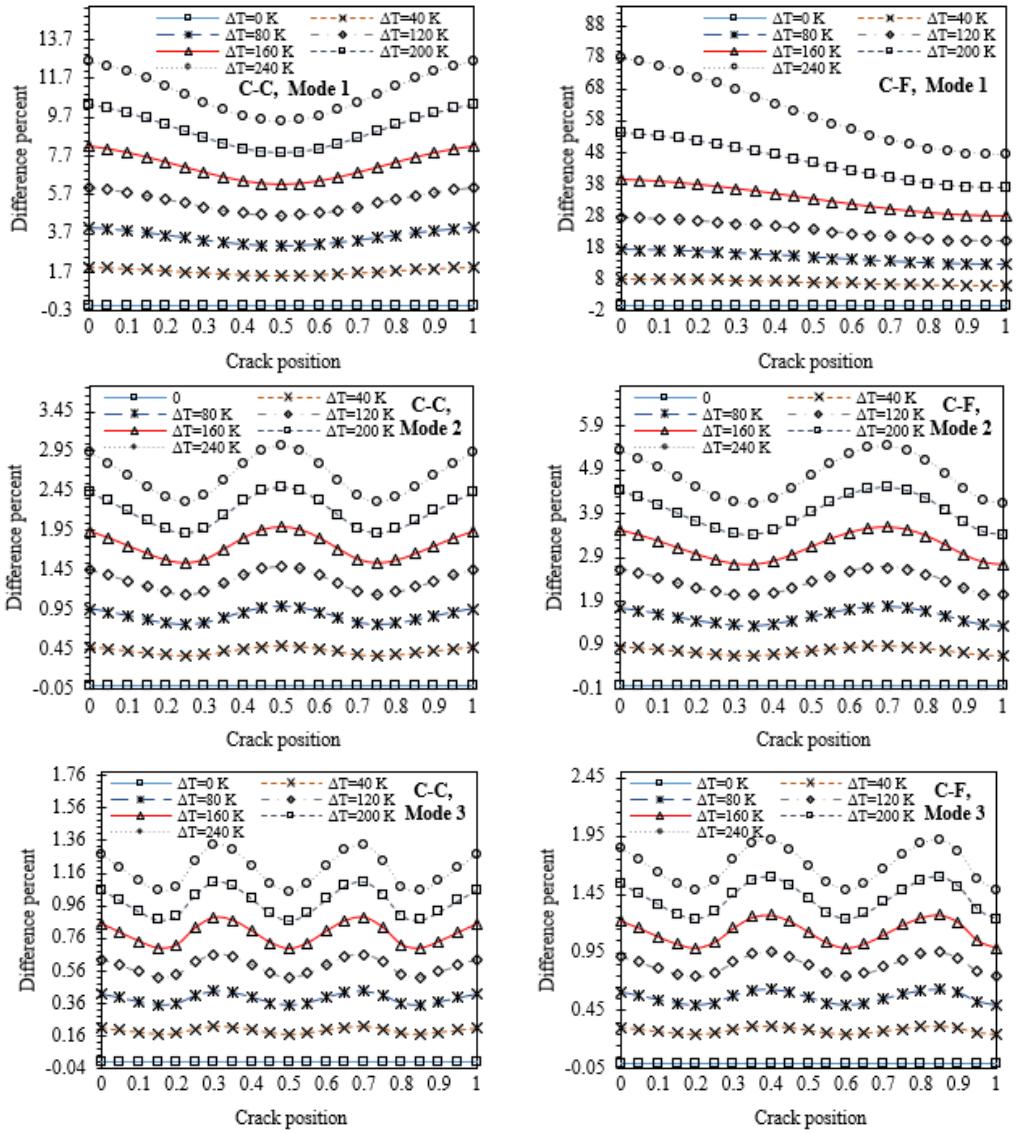

Fig. 6 Difference percent of first three modes of cracked C-C and C-F nanorods with different crack positions (b) at room temperature or higher ($K_t = 0,\ L = 20\ nm,\ e_o a = 2\ nm$, and $C_s = 0.15$)

Table 6 First three dimensionless frequencies of a cracked C-F nanorod with different nonlocal scale coefficients and crack severities at room temperature or higher ($K_t = 0,\ L = 20\ nm$, and $b = 0.25$)

$e_o a\ (nm)$	$\Delta T\ (K)$	$C_s = 0$			$C_s = 0.15$			$C_s = 0.35$		
		λ_1	λ_2	λ_3	λ_1	λ_2	λ_3	λ_1	λ_2	λ_3
0	0	1.5708	4.7124	7.8540	1.3990	4.6228	7.6533	1.2352	4.5378	7.3606
	40	1.4734	4.6806	7.8346	1.2887	4.5904	7.6335	1.1088	4.5048	7.3399
	120	1.2562	4.6162	7.7957	1.0335	4.5248	7.5936	0.7980	4.4379	7.2985
	200	0.9925	4.5510	7.7566	0.6894	4.4583	7.5535	0.2101	4.3701	7.2569
0.5	0	1.5696	4.6800	7.7068	1.3982	4.5923	7.5170	1.2347	4.5089	7.2390
	40	1.4723	4.6484	7.6878	1.2880	4.5600	7.4975	1.1083	4.4760	7.2187
	120	1.2552	4.5845	7.6496	1.0328	4.4949	7.4583	0.7976	4.4097	7.1780
	200	0.9918	4.5197	7.6113	0.6890	4.4288	7.4189	0.2100	4.3422	7.1370
1	0	1.5660	4.5868	7.3105	1.3956	4.5041	7.1479	1.2329	4.4253	6.9076
	40	1.4689	4.5558	7.2925	1.2856	4.4725	7.1293	1.1067	4.3931	6.8883
	120	1.2523	4.4932	7.2562	1.0310	4.4086	7.0921	0.7965	4.3279	6.8494
	200	0.9895	4.4297	7.2198	0.6877	4.3437	7.0546	0.2097	4.2618	6.8103

Table 6 Continued

$e_o a\ (nm)$	$\Delta T\ (K)$	$C_s = 0$			$C_s = 0.15$			$C_s = 0.35$		
		λ_1	λ_2	λ_3	λ_1	λ_2	λ_3	λ_1	λ_2	λ_3
1.5	0	1.5600	4.4431	6.7672	1.3914	4.3678	6.6376	1.2300	4.2958	6.4439
	40	1.4633	4.4130	6.7505	1.2817	4.3371	6.6204	1.1041	4.2645	6.4258
	120	1.2476	4.3524	6.7170	1.0278	4.2751	6.5858	0.7946	4.2013	6.3896
	200	0.9857	4.2909	6.6833	0.6856	4.2123	6.5510	0.2092	4.1371	6.3531
2	0	1.5518	4.2628	6.1767	1.3855	4.1962	6.0776	1.2259	4.1323	5.9279
	40	1.4556	4.2340	6.1614	1.2763	4.1667	6.0619	1.1005	4.1022	5.9113
	120	1.2410	4.1758	6.1308	1.0235	4.1072	6.0302	0.7920	4.0413	5.8779
	200	0.98051	4.1168	6.1001	0.6828	4.0468	5.9984	0.2085	3.9795	5.8444

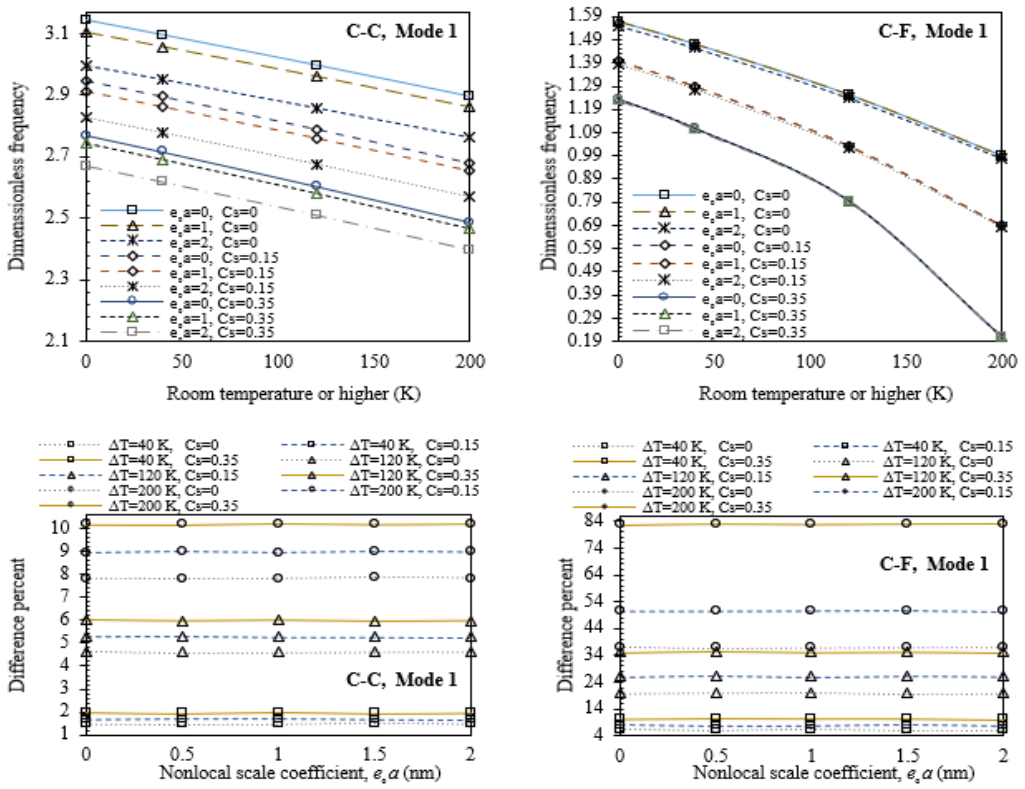

Fig.7 Frequency and difference percent of the first mode of C-C and C-F nanorods with different nonlocal scale coefficients and crack severities at room temperature or higher ($K_t = 0$ and $L = 20\ nm$, and $b = 0.25$)

Table 7 First three dimensionless frequencies of a cracked C-C nanorod with different elastic medium stiffness and crack severities at room temperature or higher ($L = 20\ nm$, $e_o a = 2\ nm$, and $b = 0.25$)

$K_t(nN)$	$\Delta T\ (K)$	$C_s = 0$			$C_s = 0.15$			$C_s = 0.35$		
		λ_1	λ_2	λ_3	λ_1	λ_2	λ_1	λ_2	λ_3	λ_3
0	0	2.9972	5.3202	6.8587	2.8253	5.3202	6.5380	2.6701	5.3202	6.1900
	40	2.9517	5.2998	6.8468	2.7765	5.2998	6.5245	2.6179	5.2998	6.1748
	120	2.8585	5.2589	6.8230	2.6762	5.2589	6.4977	2.5103	5.2589	6.1444
	200	2.7622	5.2177	6.7990	2.5719	5.2177	6.4707	2.3978	5.2177	6.1138
0.5	0	3.6570	5.7180	7.1716	3.5175	5.7180	6.8655	3.3941	5.7180	6.5350
	40	3.6198	5.6990	7.1602	3.4785	5.6990	6.8528	3.3532	5.6990	6.5207
	120	3.5442	5.6610	7.1375	3.3989	5.6610	6.8272	3.2699	5.6610	6.4918
	200	3.4670	5.6227	7.1146	3.3175	5.6227	6.8015	3.1844	5.6227	6.4629

Table 7 Continued

$K_t(nN)$	$\Delta T\ (K)$	C_s = 0			C_s = 0.15			C_s = 0.35		
		λ_1	λ_2	λ_3	λ_1	λ_2	λ_1	λ_2	λ_3	λ_3
1	0	4.2148	6.0898	7.4715	4.0944	6.0898	7.1782	3.9888	6.0898	6.8628
	40	4.1826	6.0720	7.4606	4.0608	6.0720	7.1660	3.9541	6.0720	6.8491
	120	4.1173	6.0364	7.4387	3.9929	6.0364	7.1415	3.8837	6.0364	6.8216
	200	4.0510	6.0005	7.4168	3.9238	6.0005	7.1169	3.8120	6.0005	6.7941
1.5	0	4.7069	6.4402	7.7597	4.5994	6.4402	7.4778	4.5057	6.4402	7.1755
	40	4.6781	6.4234	7.7492	4.5696	6.4234	7.4660	4.4750	6.4234	7.1624
	120	4.6199	6.3897	7.7282	4.5093	6.3897	7.4426	4.4129	6.3897	7.1362
	200	4.5609	6.3558	7.7071	4.4483	6.3558	7.4190	4.3499	6.3558	7.1099
2	0	5.1523	6.7725	8.0377	5.0542	6.7725	7.7658	4.9691	6.7725	7.4752
	40	5.1259	6.7566	8.0275	5.0271	6.7566	7.7545	4.9413	6.7566	7.4627
	120	5.0728	6.7245	8.0072	4.9724	6.7245	7.7319	4.8851	6.7245	7.4375
	200	5.0192	6.6923	7.9868	4.9171	6.6923	7.7092	4.8283	6.6923	7.4122

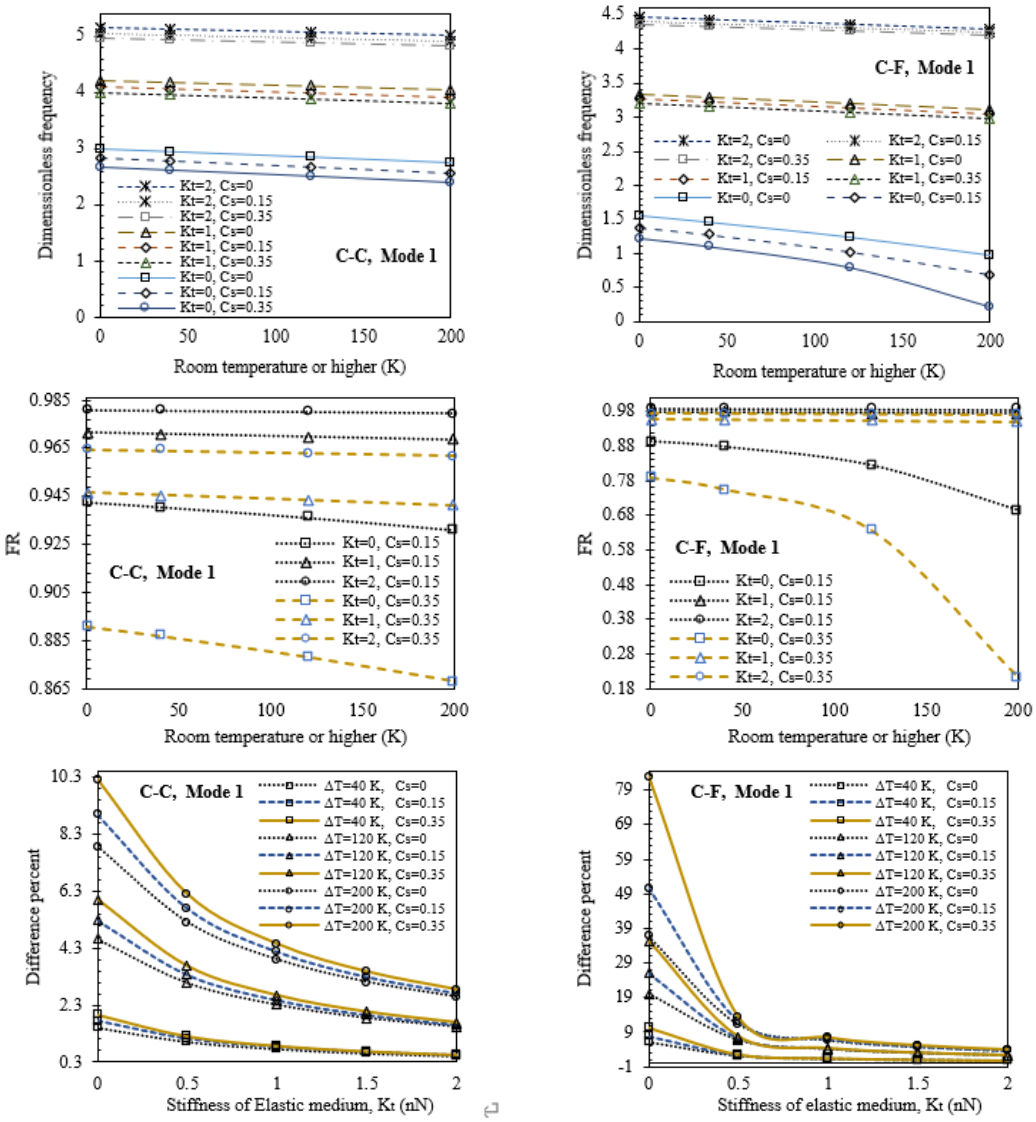

Fig. 8 Frequency, frequency ratio, and difference percent of the first mode of C-C and C-F nanorods with different elastic medium stiffness and crack severities at room temperature or higher. ($L = 20\ nm, e_o a = 2\ nm,$ and $b = 0.25$)

Table 8 First three dimensionless frequencies of a cracked C-F nanorod with different lengths and crack severities at room temperature or higher ($K_t = 0,\ e_o a = 2\ nm$, and $b = 0.25$)

$L(nm)$	$\Delta T\ (K)$	C_s = 0			C_s = 0.15			C_s = 0.35		
		λ_1	λ_2	λ_3	λ_1	λ_2	λ_1	λ_2	λ_3	λ_3
5	0	1.3300	2.2085	2.3822	1.2209	2.1990	2.3764	1.1074	2.1897	2.3672
	40	1.3250	2.2074	2.3817	1.2150	2.1979	2.3759	1.1006	2.1886	2.3666
	120	1.3147	2.2053	2.3807	1.2032	2.1957	2.3748	1.0869	2.1863	2.3655
	200	1.3044	2.2031	2.3797	1.1912	2.1936	2.3738	1.0730	2.1840	2.3644
10	0	1.4986	3.4293	4.2178	1.3473	3.3944	4.1859	1.1992	3.3603	4.1360
	40	1.4758	3.4234	4.2150	1.3215	3.3883	4.1830	1.1697	3.3540	4.1329
	120	1.4292	3.4115	4.2094	1.2682	3.3760	4.1771	1.1082	3.3414	4.1267
	200	1.3811	3.3995	4.2038	1.2127	3.3637	4.1713	1.0432	3.3288	4.1205
15	0	1.5374	3.9901	5.4241	1.3753	3.9353	5.3567	1.2188	3.8825	5.2533
	40	1.4845	3.9749	5.4164	1.3154	3.9197	5.3487	1.1503	3.8665	5.2449
	120	1.3726	3.9442	5.4011	1.1865	3.8883	5.3328	0.9992	3.8343	5.2280
	200	1.2507	3.9133	5.3856	1.0418	3.8566	5.3167	0.8208	3.8019	5.2111
20	0	1.5518	4.2628	6.1767	1.3855	4.1962	6.0776	1.2259	4.1323	5.9279
	40	1.4556	4.2340	6.1614	1.2763	4.1667	6.0619	1.1005	4.1022	5.9113
	120	1.2410	4.1758	6.1308	1.0235	4.1072	6.0302	0.7920	4.0413	5.8779
	200	0.98051	4.1168	6.1001	0.6828	4.0468	5.9984	0.2085	3.9795	5.8444
25	0	1.5585	4.4095	6.6502	1.3903	4.3358	6.5271	1.2293	4.2654	6.3426
	40	1.4047	4.3630	6.6248	1.2148	4.2883	6.5008	1.0260	4.2170	6.3151
	120	1.0303	4.2685	6.5737	0.7492	4.1918	6.4480	0.3684	4.1183	6.2596
	200	0.38711	4.1719	6.5221	…	4.0929	6.3947	…	4.0172	6.2036

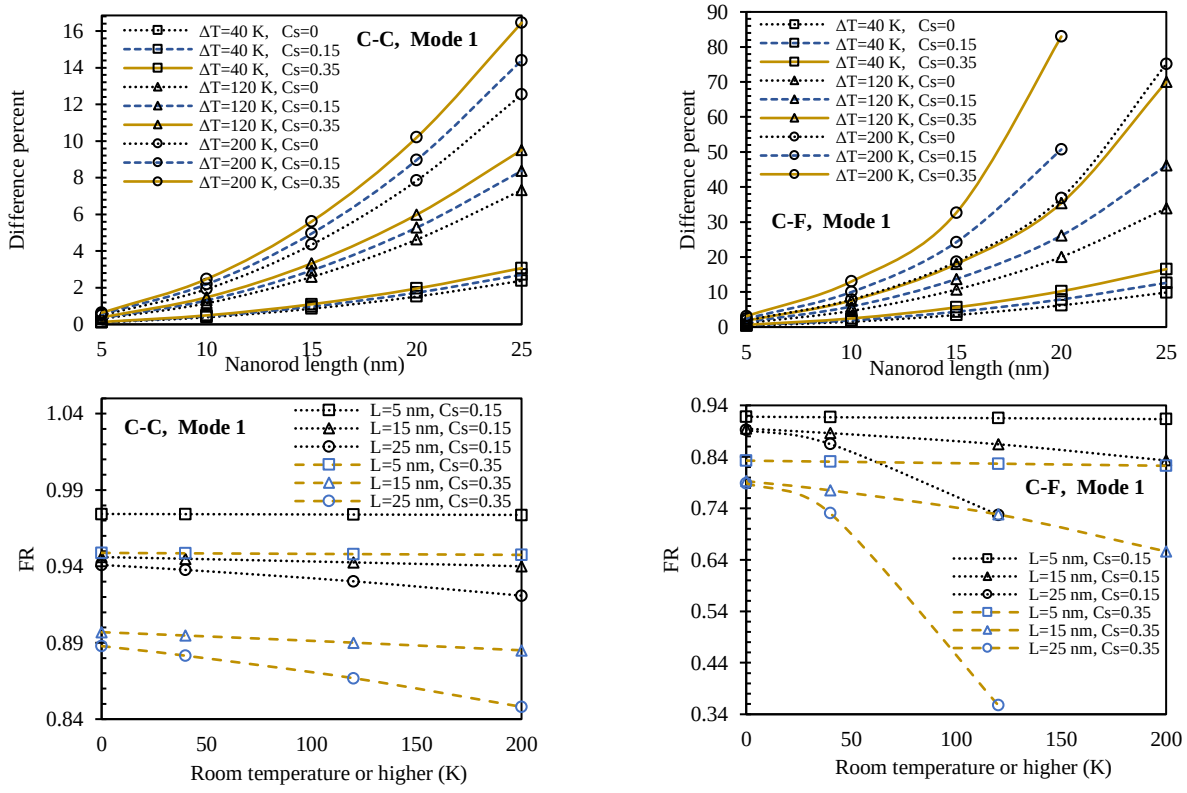

Fig. 9 Difference percent and frequency ratio of the first mode of C-C and C-F nanorods with different lengths and crack severities at room temperature or higher ($K_t = 0,\ e_o a = 2\ nm,\ b = 0.25$)

Table 9 First three dimensionless frequencies of a double-cracked C-C nanorod with different positions of the second crack and crack severities at room temperature or higher ($L = 20\,nm$, $e_o a = 2\,nm$, and $b_1 = 0.25$)

b_2	ΔT (K)	$K_t = 0$						$K_t = 0.5\,(nN)$					
		$C_s = 0.15$			$C_s = 0.35$			$C_s = 0.15$			$C_s = 0.35$		
		λ_1	λ_2	λ_3	λ_1	λ_2	λ_3	λ_1	λ_2	λ_3	λ_1	λ_2	λ_3
0.1	0	2.580	5.062	6.535	2.314	4.909	6.075	3.323	5.478	6.863	3.121	5.338	6.427
	40	2.525	5.040	6.522	2.252	4.886	6.060	3.281	5.458	6.850	3.076	5.316	6.412
	80	2.470	5.017	6.509	2.189	4.862	6.044	3.239	5.437	6.838	3.030	5.295	6.397
	120	2.413	4.995	6.495	2.124	4.839	6.028	3.196	5.417	6.825	2.983	5.273	6.382
0.25	0	2.703	5.320	6.261	2.506	5.320	5.878	3.420	5.718	6.602	3.267	5.718	6.240
	40	2.651	5.299	6.246	2.450	5.299	5.861	3.379	5.699	6.588	3.224	5.699	6.224
	80	2.599	5.279	6.231	2.393	5.279	5.844	3.338	5.680	6.574	3.180	5.680	6.208
	120	2.545	5.258	6.216	2.334	5.258	5.827	3.297	5.661	6.560	3.136	5.661	6.192
0.5	0	2.821	4.802	6.498	2.638	4.296	6.088	3.514	5.239	6.827	3.369	4.780	6.438
	40	2.772	4.778	6.484	2.585	4.267	6.072	3.475	5.217	6.814	3.328	4.754	6.424
	80	2.722	4.754	6.471	2.531	4.239	6.056	3.435	5.195	6.801	3.286	4.728	6.409
	120	2.672	4.730	6.457	2.476	4.210	6.041	3.395	5.173	6.788	3.244	4.703	6.394
0.6	0	2.769	4.954	6.320	2.510	4.587	5.969	3.472	5.379	6.659	3.270	5.043	6.327
	40	2.719	4.931	6.306	2.454	4.561	5.953	3.432	5.358	6.645	3.227	5.019	6.311
	80	2.668	4.908	6.291	2.397	4.535	5.937	3.392	5.337	6.631	3.183	4.996	6.296
	120	2.616	4.885	6.277	2.338	4.509	5.920	3.352	5.316	6.617	3.138	4.972	6.280
0.8	0	2.598	5.273	6.528	2.235	5.230	6.190	3.337	5.674	6.856	3.063	5.634	6.535
	40	2.544	5.253	6.514	2.171	5.209	6.174	3.296	5.655	6.843	3.017	5.615	6.520
	80	2.489	5.232	6.501	2.105	5.188	6.159	3.253	5.636	6.830	2.970	5.595	6.506
	120	2.433	5.211	6.487	2.037	5.167	6.144	3.211	5.617	6.817	2.922	5.575	6.491

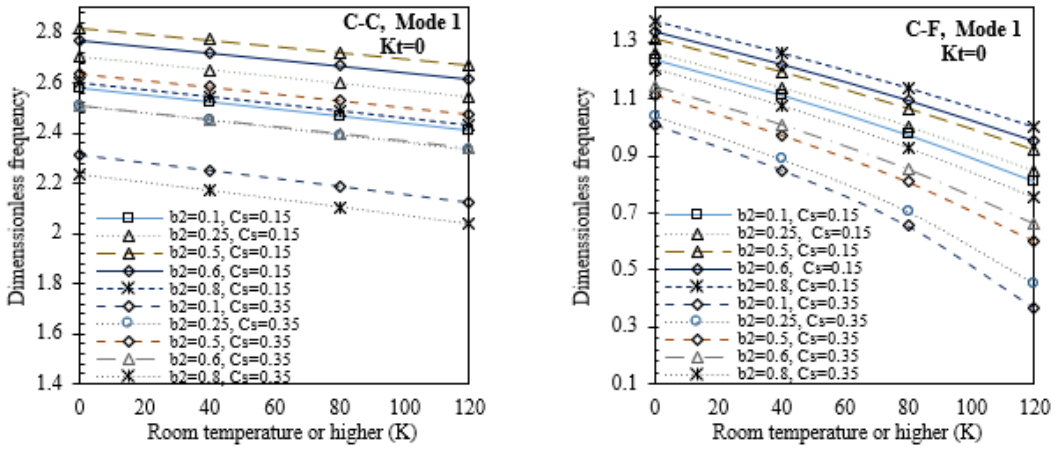

Fig. 10 First frequency of double-cracked C-C and C-F nanorods with different second crack positions and crack severities at room temperature or higher ($K_t = 0$, $L = 20\,nm$, $e_o a = 2\,nm$, and $b_1 = 0.25$)

nanorod length leads to an increase in the temperature influence (difference percent) on the torsional frequencies of the cracked C-C and C-F nanorods. The longer nanorod causes an increase in the crack effect on the frequencies as the results of Table 8 imply. The rate of reduction of the frequencies due to a crack or more can be reduced by decreasing the length of the nanorod. It can be stated that both crack and high temperature effects decrease on short SWCNTs/nanorods compared to the long ones. The frequency ratio approaches a minimum value when both nanorod length and crack severity increase for the C-C and C-F nanorods.

The double-cracked C-C nanorod frequencies with and without elastic medium for various crack severities at room temperature or higher for the various second crack positions are tabulated in Table 9. The presence of the second crack leads to less torsional stiffness than a single crack. As Fig. 10 shows, the first mode of the C-C nanorod possesses its

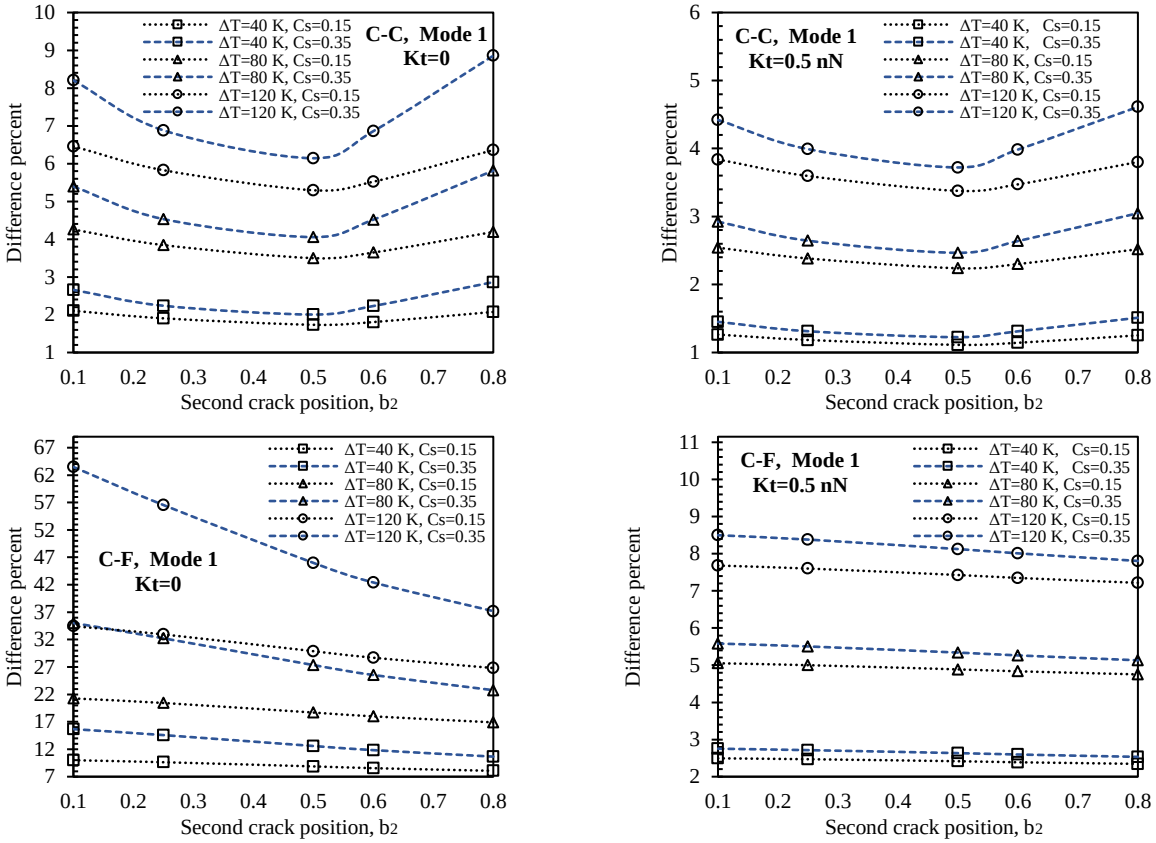

(a) $K_t = 0$ (b) $K_t = 0.5\ (nN)$

Fig. 11 Difference percent of the first mode of double-cracked C-C and C-F nanorods with different second crack positions and crack severities with and without elastic medium at room temperature or higher ($L = 20\ nm,\ e_o a = 2\ nm$, and $b_1 = 0.25$)

maximum value when the second crack locates on the nanorod middle point and for the C-F nanorod, the maximum value of the first mode belongs to the crack location of $b_2 = 0.8$. The frequencies of all modes of both nanorod types decrease with an increase in temperature for any second crack location. By comparing the cases of the presence and absence of the elastic medium for the double-cracked nanorods, it is observed that the difference percent significantly decreases due to the presence of the elastic medium at any second crack position. The highest difference percent of the C-C and C-F nanorods occurs when the second crack approaches or locates on the fixed ends as shown in Fig. 11.

4. Conclusions

The following points are concluded according to the presented results and discussions:

• The torsional frequencies of non-cracked and cracked nanorods decrease at the high temperatures for any crack location and any crack severity.

• At temperatures lower than the room temperature, all frequencies of any boundary condition increase for any crack location and any crack severity.

• An increase in the crack severity leads to a decrease in all frequencies at any temperature.

• The crack location influences the effect of the temperature changes on the frequencies. At some crack locations, some modes of the C-C rod are independent of the crack because of the symmetry in the boundary condition.

• The presence of the elastic medium decreases the effect of the crack and high temperatures on the frequencies.

• Increasing the nanorod length results in an increase in the torsional frequencies for any crack severity and any temperature.

• The double-cracked nanorods are more impressed by the temperature compared to the non or single-cracked cases. The frequencies of double-cracked nanorods are lower than non or single-cracked cases.

• The difference percent or effect of the temperature changes on the frequencies decreases with an increase in the elastic medium stiffness. It increases with increasing the crack severity and nanorod length and it is independent of the nonlocal scale coefficient. The effect of the crack location on the difference percent depends on the vibration mode and boundary conditions.

Funding sources

This research did not receive any specific grant from

funding agencies in the public, commercial, or not-for-profit sectors.

Acknowledgments

The authors are grateful to the Iran University of Science and Technology and the University of Salahaddin-Erbil for supporting this work.

References

Abdullah, S.S., Hosseini-Hashemi, S., Hussein, N.A. and Nazemnezhad, R. (2020a), "Effect of temperature on vibration of cracked single-walled carbon nanotubes embedded in an elastic medium under different boundary conditions", *Mech. Based Des. Struct.*, 1-26. https://doi.org/10.1080/15397734.2020.1759431.

Abdullah, S.S., Hosseini-Hashemi, S., Hussein, N.A. and Nazemnezhad, R. (2020b), "Thermal stress and magnetic effects on nonlinear vibration of nanobeams embedded in nonlinear elastic medium", *J. Therm. Stress.*, **43**(10), 1316-1332. https://doi.org/10.1080/01495739.2020.1780175.

Abdullah, S.S., Hosseini-Hashemi, S., Hussein, N.A. and Nazemnezhad, R. (2020c), "Temperature change effect on torsional vibration of nanorods embedded in an elastic medium using Rayleigh–Ritz method", *J. Brazil. Soc. Mech. Sci. Eng.*, **42**(11), 1-20. https://doi.org/10.1007/s40430-020-02664-0.

Akbaş, Ş.D. (2017), "Free vibration of edge cracked functionally graded microscale beams based on the modified couple stress theory", *Int. J. Struct. Stabil. Dyn.*, **17**(3), 1750033. https://doi.org/10.1142/S021945541750033X.

Akbas, S.D. (2018), "Forced vibration analysis of cracked functionally graded microbeams", *Adv. Nano Res.*, **6**(1), 39-55. https://doi.org/10.12989/anr.2018.6.1.039.

Akgoz, B. and Civalek, O. (2011), "Nonlinear vibration analysis of laminated plates resting on nonlinear two-parameters elastic foundations", *Steel Compos. Struct.*, **11**(5), 403-421. https://doi.org/10.12989/scs.2011.11.5.403.

Apuzzo, A., Barretta, R., Luciano, R., de Sciarra, F.M. and Penna, R. (2017), "Free vibrations of Bernoulli-Euler nano-beams by the stress-driven nonlocal integral model", *Compos. Part B Eng.*, **123**, 105-111. https://doi.org/10.1016/j.compositesb.2017.03.057.

Azrar, A., Azrar, L. and Aljinaidi, A.A. (2016), "Analytical and numerical modeling of higher order free vibration characteristics of single-walled carbon nanotubes", *Mech. Adv. Mater. Struct.*, **23**(11), 1245-1262. https://doi.org/10.1080/15376494.2015.1068405.

Barretta, R., Faghidian, S.A. and Luciano, R. (2019), "Longitudinal vibrations of nano-rods by stress-driven integral elasticity", *Mech. Adv. Mater. Struct.*, **26**(15), 1307-1315. https://doi.org/10.1080/15376494.2018.1432806.

Berghouti, H., Adda Bedia, E., Benkhedda, A. and Tounsi, A. (2019), "Vibration analysis of nonlocal porous nanobeams made of functionally graded material", *Adv. Nano Res.*, **7**(5), 351-364. https://doi.org/10.12989/anr.2019.7.5.351.

Berrabah, H., Tounsi, A., Semmah, A. and Adda Bedia, E. (2013), "Comparison of various refined nonlocal beam theories for bending, vibration and buckling analysis of nanobeams", *Struct. Eng. Mech.*, **48**(3), 351-365. https://doi.org/10.12989/sem.2013.48.3.351.

Demir, Ç. and Civalek, Ö. (2017), "A new nonlocal FEM via Hermitian cubic shape functions for thermal vibration of nano beams surrounded by an elastic matrix", *Compos. Struct.*, **168**, 872-884. https://doi.org/10.1016/j.compstruct.2017.02.091.

Donà, M., Palmeri, A. and Lombardo, M. (2015), "Dynamic analysis of multi-cracked Euler–Bernoulli beams with gradient elasticity", *Comput. Struct.*, **161**, 64-76. https://doi.org/10.1016/j.compstruc.2015.08.013.

Duc, N.D. (2016), "Nonlinear thermal dynamic analysis of eccentrically stiffened S-FGM circular cylindrical shells surrounded on elastic foundations using the Reddy's third-order shear deformation shell theory", *Eur. J. Mech. A Solids*, **58**, 10-30. https://doi.org/10.1016/j.euromechsol.2016.01.004.

Ebrahimi, F. and Mahmoodi, F. (2018), "Vibration analysis of carbon nanotubes with multiple cracks in thermal environment", *Adv. Nano Res.*, **6**(1), 57-80. https://doi.org/10.12989/anr.2018.6.1.057.

Ebrahimi, F., Daman, M. and Mahesh, V. (2019), "Thermo-mechanical vibration analysis of curved imperfect nano-beams based on nonlocal strain gradient theory", *Adv. Nano Res.*, **7**(4), 249-263. https://doi.org/10.12989/anr.2019.7.4.249.

Eringen, A.C. and Edelen, D. (1972), "On nonlocal elasticity", *Int. J. Eng. Sci.*, **10**(3), 233-248. https://doi.org/10.1016/0020-7225(72)90039-0.

Fazelzadeh, S. and Pouresmaeeli, S. (2013), "Thermo-mechanical vibration of double-orthotropic nanoplates surrounded by elastic medium", *J. Therm. Stress.*, **36**(3), 225-238. https://doi.org/10.1080/01495739.2013.765170.

Hosseini-Hashemi, S., Nazemnezhad, R. and Rokni, H. (2015), "Nonlocal nonlinear free vibration of nanobeams with surface effects", *Eur. J. Mech. A Solid*, **52**, 44-53. https://doi.org/10.1016/j.euromechsol.2014.12.012.

Hussein, N.A., Rasul, H.A. and Abdullah, S.S. (2020), "The free vibration analysis of multi-cracked nanobeam using nonlocal elasticity theory", *Zanco J. Pure Appl. Sci.*, **32**(2), 39-54. https://doi.org/10.21271/ZJPAS.32.2.5.

Khorshidi, M.A. and Shariati, M. (2016), "Free vibration analysis of sigmoid functionally graded nanobeams based on a modified couple stress theory with general shear deformation theory", , *J. Brazil. Soc. Mech. Sci. Eng.*, **38**(8), 2607-2619. https://doi.org/10.1007/s40430-015-0388-3.

Loya, J., Aranda-Ruiz, J.A. and Fernández-Sáez, J. (2014), "Torsion of cracked nanorods using a nonlocal elasticity model", *J. Phys. D Appl. Phys.*, **47**(11), 115304. https://doi.org/10.1088/0022-3727/47/11/115304.

Loya, J., López-Puente, J., Zaera, R. and Fernández-Sáez, J. (2009), "Free transverse vibrations of cracked nanobeams using a nonlocal elasticity model", *J. Appl. Phys.*, **105**(4), 044309. https://doi.org/10.1063/1.3068370.

Lu, J.P. (1997), "Elastic properties of single and multilayered nanotubes", *J. Phys. Chem. Solid*, **58**(11), 1649-1652. https://doi.org/10.1016/S0022-3697(97)00045-0.

Ma'en, S.S. (2017), "Superharmonic resonance analysis of nonlocal nano beam subjected to axial thermal and magnetic forces and resting on a nonlinear elastic foundation", *Microsyst. Technol.*, **23**(8), 3319-3330. https://doi.org/10.1007/s00542-016-3161-3.

Mehta, V. and Kumar, S. (1994), "Temperature dependent torsional properties of high performance fibres and their relevance to compressive strength", *J. Mater. Sci.*, **29**(14), 3658-3664. https://doi.org/10.1007/BF00357332.

Nazemnezhad, R. and Fahimi, P. (2017), "Free torsional vibration of cracked nanobeams incorporating surface energy effects", *Appl. Math. Mech.*, **38**(2), 217-230. https://doi.org/10.1007/s10483-017-2167-9.

Nazemnezhad, R., Mahoori, R. and Samadzadeh, A. (2019), "Surface energy effect on nonlinear free axial vibration and internal resonances of nanoscale rods", *Eur. J. Mech. A Solids*, **77**, 103784. https://doi.org/10.1016/j.euromechsol.2019.05.001.

Numanoğlu, H.M. and Civalek, Ö. (2019), "On the torsional

vibration of nanorods surrounded by elastic matrix via nonlocal FEM", *Int. J. Mech. Sci.*, **161**, 105076. https://doi.org/10.1016/j.ijmecsci.2019.105076.

Polizzotto, C. (2014), "Stress gradient versus strain gradient constitutive models within elasticity", *Int. J. Solid Struct.*, **51**(9), 1809-1818. https://doi.org/10.1016/j.ijsolstr.2014.01.021.

Polizzotto, C. (2015), "A unifying variational framework for stress gradient and strain gradient elasticity theories", *Eur. J. Mech. A Solids*, **49**, 430-440. https://doi.org/10.1016/j.euromechsol.2014.08.013.

Polizzotto, C. (2016), "Variational formulations and extra boundary conditions within stress gradient elasticity theory with extensions to beam and plate models", *Int. J. Solid Struct.*, **80**, 405-419. https://doi.org/10.1016/j.ijsolstr.2015.09.015.

Praveen, G. and Reddy, J. (1998), "Nonlinear transient thermoelastic analysis of functionally graded ceramic-metal plates", *Int. J. Solid Struct.*, **35**(33), 4457-4476. https://doi.org/10.1016/S0020-7683(97)00253-9.

Rahmani, O., Hosseini, S., Noroozi Moghaddam, M. and Fakhari Golpayegani, I. (2015), "Torsional vibration of cracked nanobeam based on nonlocal stress theory with various boundary conditions: an analytical study", *Int. J. Appl. Mech.*, **7**(3), 1550036. https://doi.org/10.1142/S1758825115500362.

Reddy, J. (2007), "Nonlocal theories for bending, buckling and vibration of beams", *Int. J. Eng. Sci.*, **45**(2-8), 288-307. https://doi.org/10.1016/j.ijengsci.2007.04.004.

Reddy, J. and Pang, S. (2008), "Nonlocal continuum theories of beams for the analysis of carbon nanotubes", *J. Appl. Phys.*, **103**(2), 023511. https://doi.org/10.1063/1.2833431.

Setoodeh, A., Rezaei, M. and Shahri, M.Z. (2016), "Linear and nonlinear torsional free vibration of functionally graded micro/nano-tubes based on modified couple stress theory", *Appl. Math. Mech.*, **37**(6), 725-740. https://doi.org/10.1007/s10483-016-2085-6.

Shakhlavi, S.J., Hosseini-Hashemi, S. and Nazemnezhad, R. (2020), "Torsional vibrations investigation of nonlinear nonlocal behaviour in terms of functionally graded nanotubes", *Int. J. Non Linear Mech.*, 103513. https://doi.org/10.1016/j.ijnonlinmec.2020.103513.

Şimşek, M. (2016), "Nonlinear free vibration of a functionally graded nanobeam using nonlocal strain gradient theory and a novel Hamiltonian approach", *Int. J. Eng. Sci.*, **105**, 12-27. https://doi.org/10.1016/j.ijengsci.2016.04.013.

Wang, Q. and Wang, C. (2007), "The constitutive relation and small scale parameter of nonlocal continuum mechanics for modelling carbon nanotubes", *Nanotechnology*, **18**(7), 075702. https://doi.org/10.1088/0957-4484/18/7/075702.

Yao, X. and Han, Q. (2006), "Buckling analysis of multiwalled carbon nanotubes under torsional load coupling with temperature change", *J. Eng. Mater. Technol.*, **128**(3), 419-427. https://doi.org/10.1115/1.2203102.

Yayli, M.Ö., Kandemir, S.Y. and Çerçevik, A.E. (2019), "Torsional vibration of cracked carbon nanotubes with torsional restraints using Eringen's nonlocal differential model", *J. Low Freq. Noise V. A.*, **38**(1), 70-87. https://doi.org/10.1177/1461348418813255.

Żur, K.K., Arefi, M., Kim, J. and Reddy, J. (2020), "Free vibration and buckling analyses of magneto-electro-elastic FGM nanoplates based on nonlocal modified higher-order sinusoidal shear deformation theory", *Compos. Part B Eng.*, **182**, 107601. https://doi.org/10.1016/j.compositesb.2019.107601.